Final Report

Puma Exploration Gold Deposit – Scoping Test Program; Exploration Puma Inc.

Reference No.: MIS-J10113

Prepared for:

Mr. Richard Thibault
Exploration Puma Inc.
175 Rue Legaré
Rimouski, QC G5L 3B9

July 26, 2022

Prepared by:

Tyson McKay
Scientist
Minerals & Industrial Services

Reviewed by:

Neri Botha, P.Eng.
Manager
Minerals & Industrial Services

INTRODUCTION

RPC was requested by Mr. Richard Thibault to conduct a scoping test program on samples from the Williams Brook property for Exploration Puma Inc. located in Saint-Quentin, NB. Puma Exploration Inc. is investigating opportunities to expand current operations. This deposit contains two types of host rock with varying degrees of gold contents, of which the following two were subjected to testing:

- HGV Rhyolite
- LGV Rhyolite

The foremost objectives of this program were to characterize each of these sample types and investigate beneficiation potential of gold. Gravity characteristics were investigated as well as base case cyanidation test work. The program included mineralogical characterization.

The following report serves to summarize details of the operating conditions under which the scoping test work was performed as well as the test results and data obtained.

PROGRAM RESULTS

Sample Preparation and Head Analyses

A total of five pallets containing nearly 3000 samples of material from the Puma Exploration gold deposit were received (see Figure 1). Selected samples (see Appendix) were split into three blends:

- HGV Rhyolite Pulp (~11kg)
- LGV Rhyolite Pulp (~9.5kg)
- LGV Rhyolite Reject (~6.5kg)

The blends were homogenized and confirmed to be passing 6 mesh before sub-sampling for head assay and mineralogical analyses test work. Head analyses on representative sub-samples for each of the blends measured the head grades as outlined in Table 1 and 2.

Figure 1: Puma Exploration Material Received.

Table 1
ICP Head Chemical Analyses on Puma Exploration Gold Deposit

ICP-OES Head Assay				ICP-OES Head Assay			
Sample:	**HGV Pulp**	**LGV Pulp**	**LGV Rejects**	**Sample:**	**HGV Pulp**	**LGV Pulp**	**LGV Rejects**
ID	**mg/kg**	**mg/kg**	**mg/kg**	**ID**	**mg/kg**	**mg/kg**	**mg/kg**
Ag	3	<0.5	<0.5	Mn	284	473	373
Al	36611	35469	55639	Mo	3	9	4
As	12	22	10	Na	11795	10810	25165
Ba	300	221	286	Nb	<10	<10	17
Be	1.3	1.9	2.1	Ni	3	10	7
Bi	<10	<10	<10	P	134	136	231
Ca	584	798	1144	Pb	663	64	51
Cd	<5	<5	<5	Sb	<10	<10	<10
Ce	68	69	104	Sc	2	3	4
Co	2	3	3	Se	<10	<10	<10
Cr	28	31	55	Sn	<10	<10	<10
Cu	44	13	13	Sr	30	32	43
Fe	14226	13784	14836	Ta	<10	<10	<10
Ga	<10	10	13	Te	<50	<50	<50
Ge	<50	<50	<50	Ti	858	917	1355
In	<50	<50	<50	Tl	<50	<50	<50
K	20668	16555	20612	V	6	12	12
La	27	28	42	W	<50	<50	<50
Li	8	11	8	Zn	544	101	66
Mg	856	1016	1187	Zr	189	236	316

Table 2
Whole Rock and Gold Head Analyses on Puma Exploration Gold Deposit

Whole Rock Analyses				Eltra CS2000 Assay			
Sample:	**HGV Pulp**	**LGV Pulp**	**LGV Rejects**	**Sample:**	**HGV Pulp**	**LGV Pulp**	**LGV Rejects**
ID	**Wt. %**	**Wt. %**	**Wt. %**	**ID**	**Wt. %**	**Wt. %**	**Wt. %**
Al_2O_3	6.92	6.70	10.52	C (Total)	0.08	0.09	0.17
BaO	0.03	0.02	0.03	S (Total)	0.03	0.01	0.01
CaO	0.08	0.11	0.16	**Fire Assay**			
Cr_2O_3	<0.01	<0.01	<0.01	**Sample:**	**HGV Pulp**	**LGV Pulp**	**LGV Rejects**
Fe_2O_3	2.03	1.97	2.12	**ID**	**mg/kg**	**mg/kg**	**mg/kg**
K_2O	2.49	1.99	2.48	Au	28.83	0.43	0.46
MgO	0.14	0.17	0.20				
MnO	0.04	0.06	0.05				
Na_2O	1.59	1.46	3.40				
P_2O_5	0.03	0.03	0.05				
SiO_2	85.47	86.23	79.35				
SrO	<0.01	<0.01	<0.01				
TiO_2	0.14	0.15	0.23				
V_2O_5	<0.01	<0.01	<0.01				
ZrO_2	0.03	0.03	0.04				
LOI 1000°C	0.79	0.94	1.25				
Total	99.79	99.88	99.88				

Size-by-Assay Analysis

A representative sub-sample of the prepared LGV Rhyolite Rejects sample was dry screened. All fractions produced were weighed and representatively sub-sampled and subjected to Au fire assay analyses. The following screen sizes were utilized: 850 µm; 600 µm; 425 µm; 300 µm; 212 µm; 150 µm; 106 µm; 75 µm; 53 µm and 38 µm. The results are summarized in Table 3 with Particle Size Distribution (PSD) curve provided in the Appendix.

Table 3
LGV Rhyolite Rejects Fractional Analysis Results

Size Fraction	Passing Size (µm)	Mass (%)	Cumulative Mass (%)	Discrete Grade	Discrete Distribution	Cumulative Grade	Cumulative Distribution
				Au (g/t)	Au (%)	Au (%)	Au (%)
-850µm + 600µm	850	57.4	100.0	0.17	31.9	0.31	100.0
-600µm + 425µm	600	5.2	42.6	0.23	3.8	0.50	68.1
-425µm + 300µm	425	4.4	37.4	0.08	1.1	0.54	64.4
-300µm + 212µm	300	3.8	33.0	0.10	1.2	0.60	63.2
-212µm + 150µm	212	2.7	29.2	0.04	0.3	0.67	62.0
-150µm + 106µm	150	4.0	26.5	0.44	5.6	0.73	61.7
-106µm + 75µm	106	9.9	22.5	0.96	30.4	0.79	56.2
-75µm + 53µm	75	9.0	12.5	0.39	11.1	0.65	25.8
-53µm + 38µm	53	2.1	3.5	0.51	3.4	1.31	14.6
-38µm	38	1.4	1.4	2.53	11.3	2.53	11.3
Calc. Head		100.0		0.31	100.0		

The results as given by Table 3 showed that the -38 µm size fraction contained 11.3 % of the total Au contents at an upgraded grade of 2.53 g/t Au and comparing the Au distribution to the mass distribution it could be seen that Au tended to upgrade to the fines. In addition, it could be seen that the prepared LGV Rhyolite Rejects sample contained 12.5 % of -75 µm fines material which contained 25.8 % of the Au.

Centrifugal Gravity Concentration Test Work

Centrifugal gravity concentration test work was conducted on representative sub-samples of the LGV Rhyolite Rejects material prepared into the following three size classes:

- 100 % Passing 1.7 mm
- 100 % Passing 1.0 mm
- 100 % Passing 0.6 mm

A bench scale Knelson concentrator, as shown in Figure 2, was utilized per sample. The aim was to evaluate the potential for recovering and upgrading Au at varying degrees of liberation.

Figure 2: Bench Scale Knelson Concentrator.

The operating conditions for the set up as indicated in Figure 2 consisted of a water flow rate of 4 L/min (1.6 psi) with a feed rate of 480 mL/min (the feed slurry contained 22% solids) and a G-force corresponding to 60G.

The results produced are provided in Table 4.

Table 4
Centrifugal Gravity Concentration Test Work Results

Sample ID	Stream	Mass (%)	Grade	Distribution
			Au (g/t)	Au (%)
-1.7mm	Conc.	5.1	3.94	30.8
	Tails	94.9	0.48	69.2
	Meas. Head		0.46	
	Calc. Head	100.0	0.66	100.0
-1.0mm	Conc.	3.9	35.00	92.0
	Tails	96.1	0.13	8.0
	Meas. Head		0.46	
	Calc. Head	100.0	1.49	100.0
-0.6mm	Conc.	3.7	13.11	77.6
	Tails	96.3	0.15	22.4
	Meas. Head		0.46	
	Calc. Head	100.0	0.63	100.0

As seen from Table 4, the LGV Rhyolite Rejects material was amenable to centrifugal gravity separation and at a grind size of 100 % passing 1.0 mm a concentrate grading at 35.00 g/t Au was produced in 3.9 % of the mass to give a recovery of 92.0 % for Au. Note that the material may be susceptible to the nugget effect as the calculated head grade in this test was 1.49 g/t Au compared to the measured 0.46 g/t Au.

Mineralogical Characterization

Representative sub-samples of the concentrates produced during centrifugal gravity concentration test work (see Table 4) were combined and homogenized in preparation for mineralogical evaluation. In addition, representative sub-samples of the HGV Rhyolite and LGV Rhyolite pulp were prepared for mineralogical analyses.

Three polished grain mounts were prepared from each of the prepared sub-samples (HGV Rhyolite; LGV Rhyolite Pulp and Combined Gravity Concentrate). Each polished mount was carbon-coated and examined with a JEOL JSM-6400 Scanning Electron Microscope (SEM), equipped with a Digital Micrograph imaging system and an EDAX Genesis energy-dispersive X-ray microanalysis system. The electron images were collected with the aid of Digital Micrograph (Gatan Inc.). Backscattered electron images of the polished grain mount provide compositional contrast. Backscattered electron intensity is a function of atomic number, such that bright areas of the image are of higher average atomic number than dark areas.

LGV Rhyolite Rejects Combined Gravity Concentrate

This sample consisted of irregular, angular fragments up to 1 mm, but most fragments were in the range of 50 µm - 200 µm. Most lithic fragments consisted of varied proportions of quartz, albite, and K-feldspar, and may also contain Fe-carbonate. Quartz was the most common mineral, with lesser albite and much less K-feldspar (see Figure 3). The K-feldspar was generally finer-grained than quartz or albite and occurred predominantly as an interstitial phase. Many fragments consisted of discrete grains of these minerals. More rarely, silicate-rich lithic fragments may also contain apatite, muscovite, rutile, zircon, or xenotime.

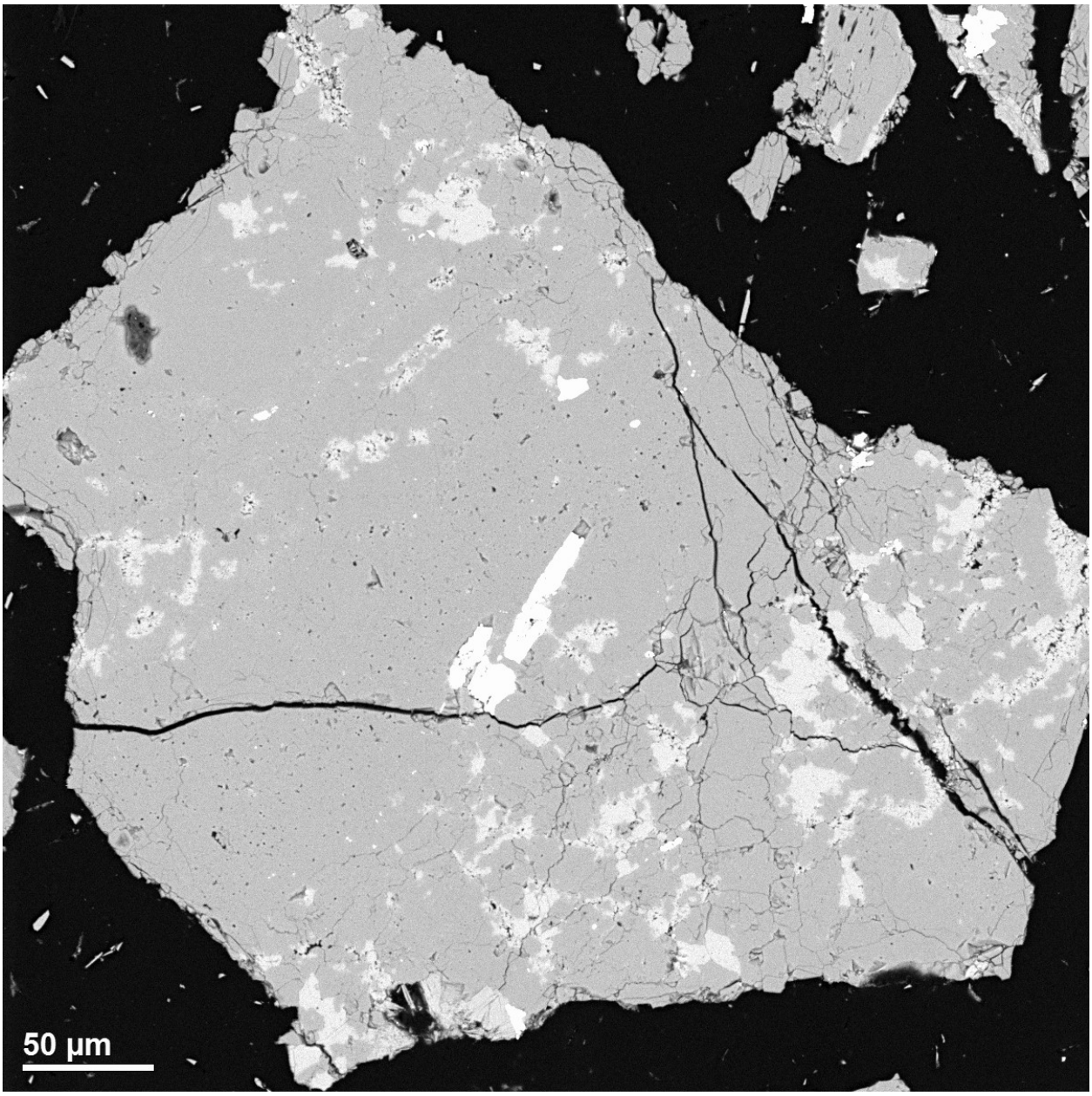

Figure 3: Silicate Fragment Consisting of K-Feldspar (Light Grey), Quartz and Albite (Medium Grey). An Elongate Apatite (White) Occurs at the Centre of the Fragment.

Sulphide mineral-rich lithic fragments were much less common than silicate fragments and were mostly small (<100 µm). These generally consisted of sphalerite, pyrite, and Fe-carbonate. More rarely, sulphide-rich fragments may contain chalcopyrite, galena, or cobaltite (see Figure 4). These sulphide minerals also occurred as discrete grain fragments. Sulphide minerals comprised less than 2% of the sample.

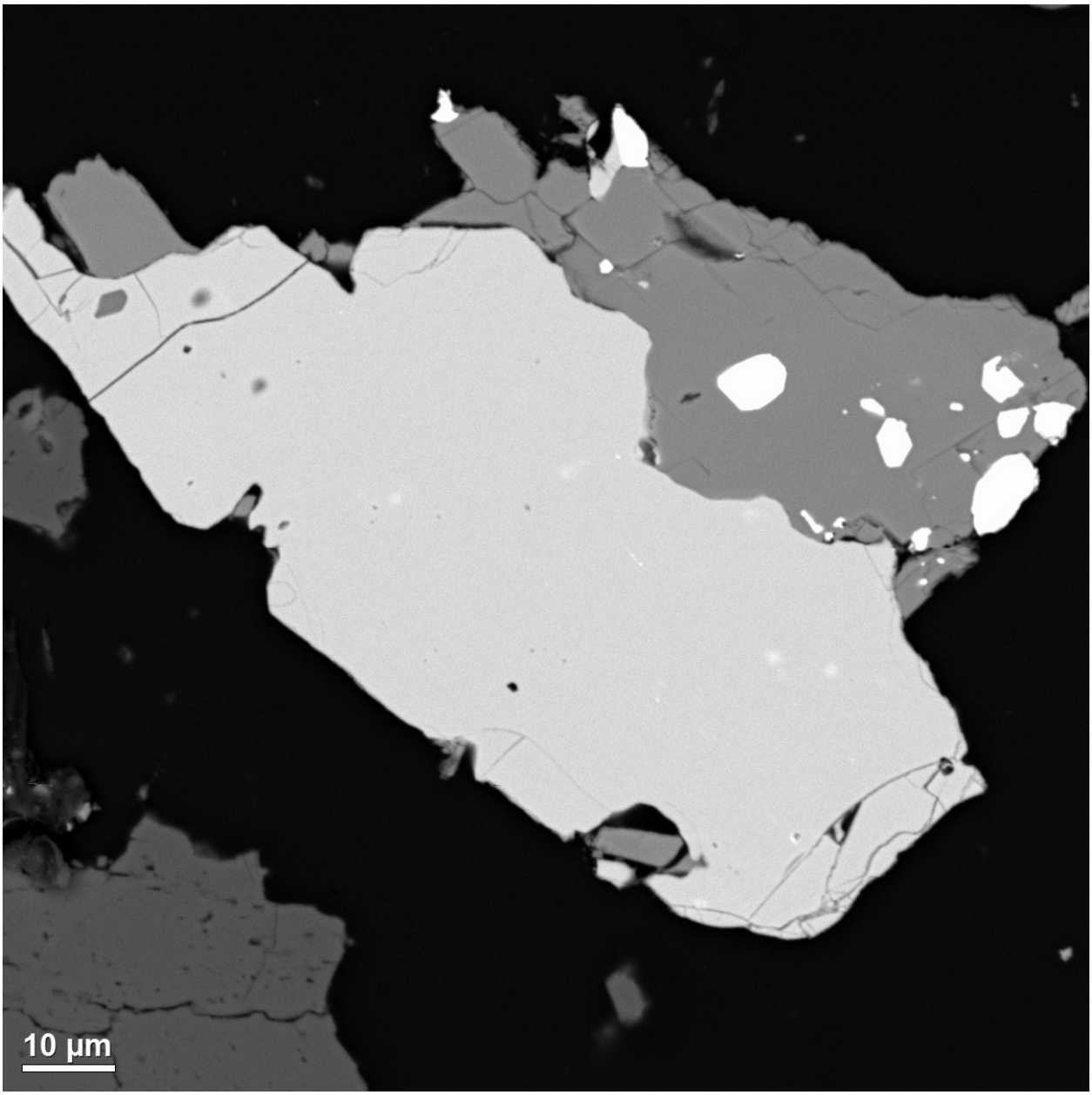

Figure 4: Fragment Consisting of Fe-Carbonate (Dark Grey) and Pyrite (Light Grey), with Inclusions of Galena and Cobaltite (White) in the Carbonate. Very Fine-Grained Inclusions of Chalcopyrite Occur in the Pyrite.

Lithic fragments with coexisting silicate and sulphide minerals had not been observed. Fe-carbonate, however, occurred in both silicate and sulphide lithic fragments.

A single fragment containing Cr-rich spinel was observed. The spinel had Cr-enriched rims and was mantled by Mg-chlorite.

Additional backscattered electron images are provided in the Appendix.

HGV Rhyolite Pulp Sample

The sample consisted mostly of discrete fragments (<100 µm), consisting of quartz, albite, or K-feldspar. These minerals constituted more than 95% of the sample (see Figure 5 and Figure 6). Muscovite, Fe-hydroxide, and Fe-carbonate were present in very minor amounts (approximately 2%). Other minerals were present in only trace quantities. Some of the largest fragments were lithic fragments, consisting of quartz, albite, and K-feldspar in varied proportions.

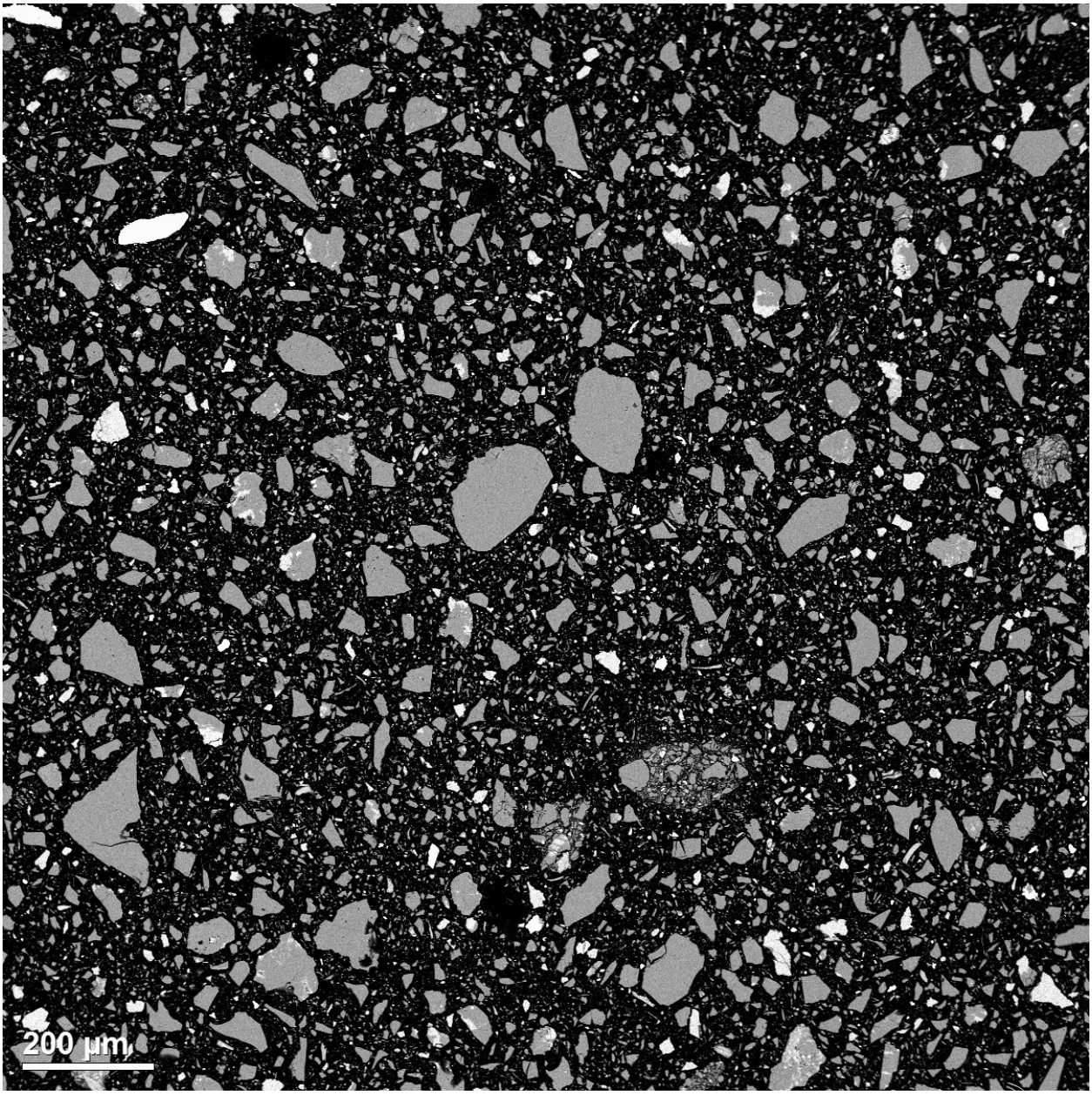

Figure 5: Low Magnification Overview.

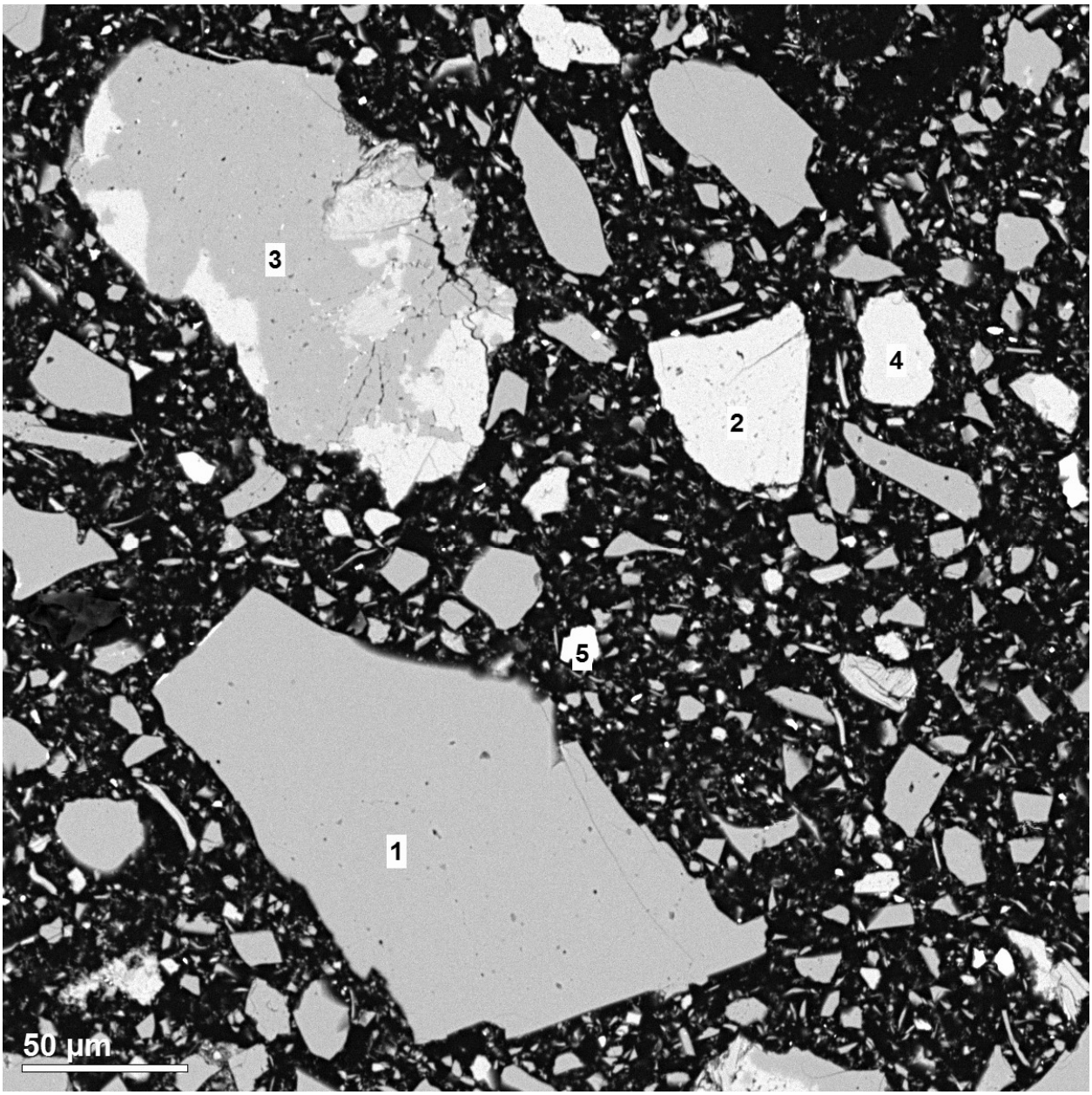

Figure 6: Fragment of 1) Quartz, 2) K-Feldspar, 3) Quartz + K-Feldspar + Albite, 4) K-Feldspar, and 5) Fe (Mg)-Carbonate.

Muscovite most commonly appeared as fine, elongate discrete grains (see Figure 7). Muscovite rarely occurred together with other phases in lithic fragments. Rutile occurred mostly as discrete fragments. Rutile grains were typically inhomogeneous, with brighter areas in backscattered electron images representing areas enriched in tungsten and niobium. Fe-hydroxide typically occurred as discrete fragments (10 µm – 20 µm). These were typically inhomogeneous and contained minor and varied amounts of Al, Si, and K. Fe-carbonate also occurred mostly as discrete grain fragments.

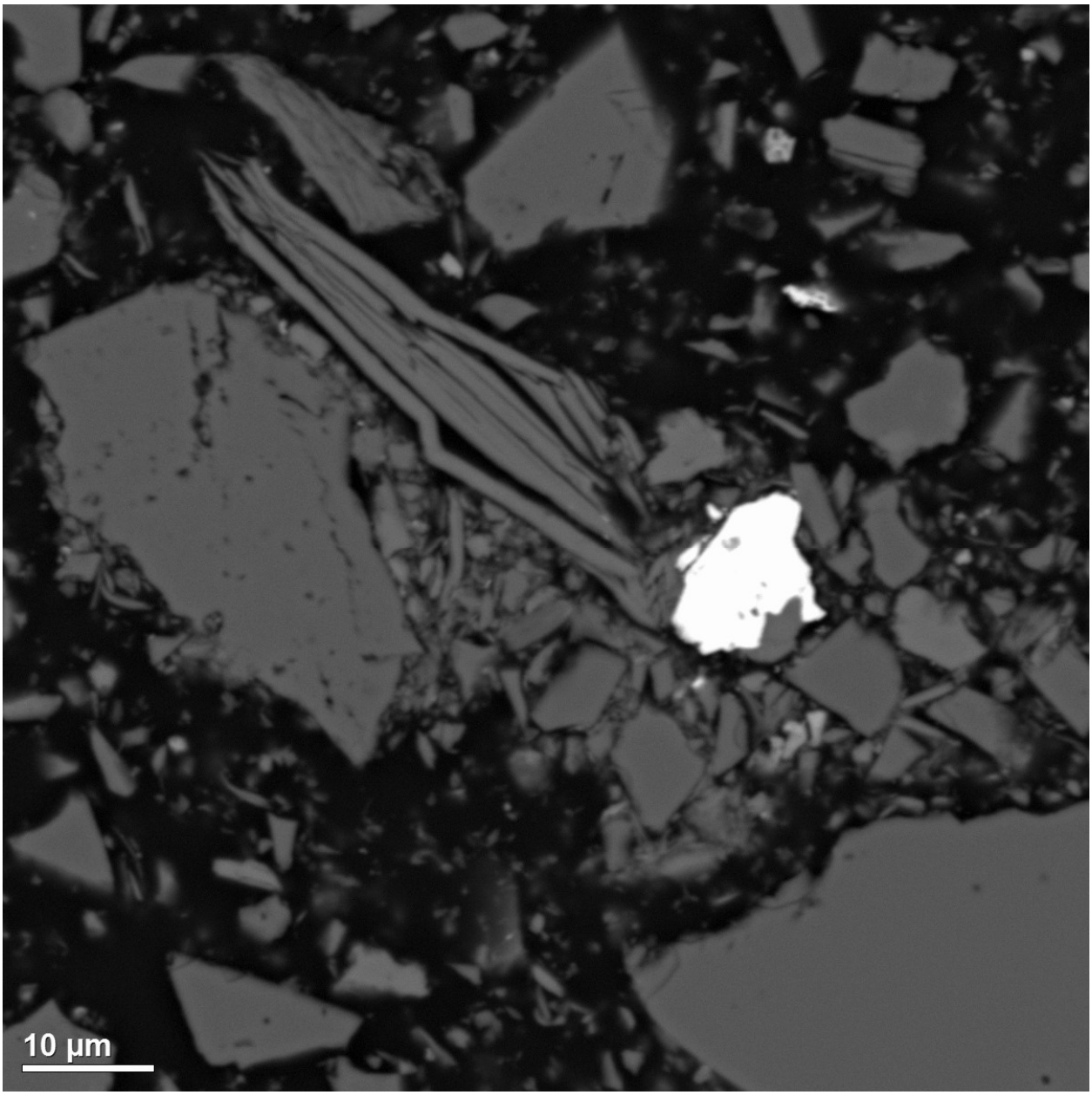

Figure 7: Elongate Muscovite Together with Monazite (White), Albite (Large Grain at Left), and Quartz (Bottom Right).

Sulphide minerals were present in trace amounts, and generally occurred as discrete fragments. Sphalerite was the most abundant of these, and commonly contained very fine inclusions of chalcopyrite. Chalcopyrite was not otherwise identified. Galena occurred as discrete grains (<10 um). One grain of electrum was identified and has a composition of approximately $Au_{80}Ag_{20}$ (atomic) as shown in Figure 8.

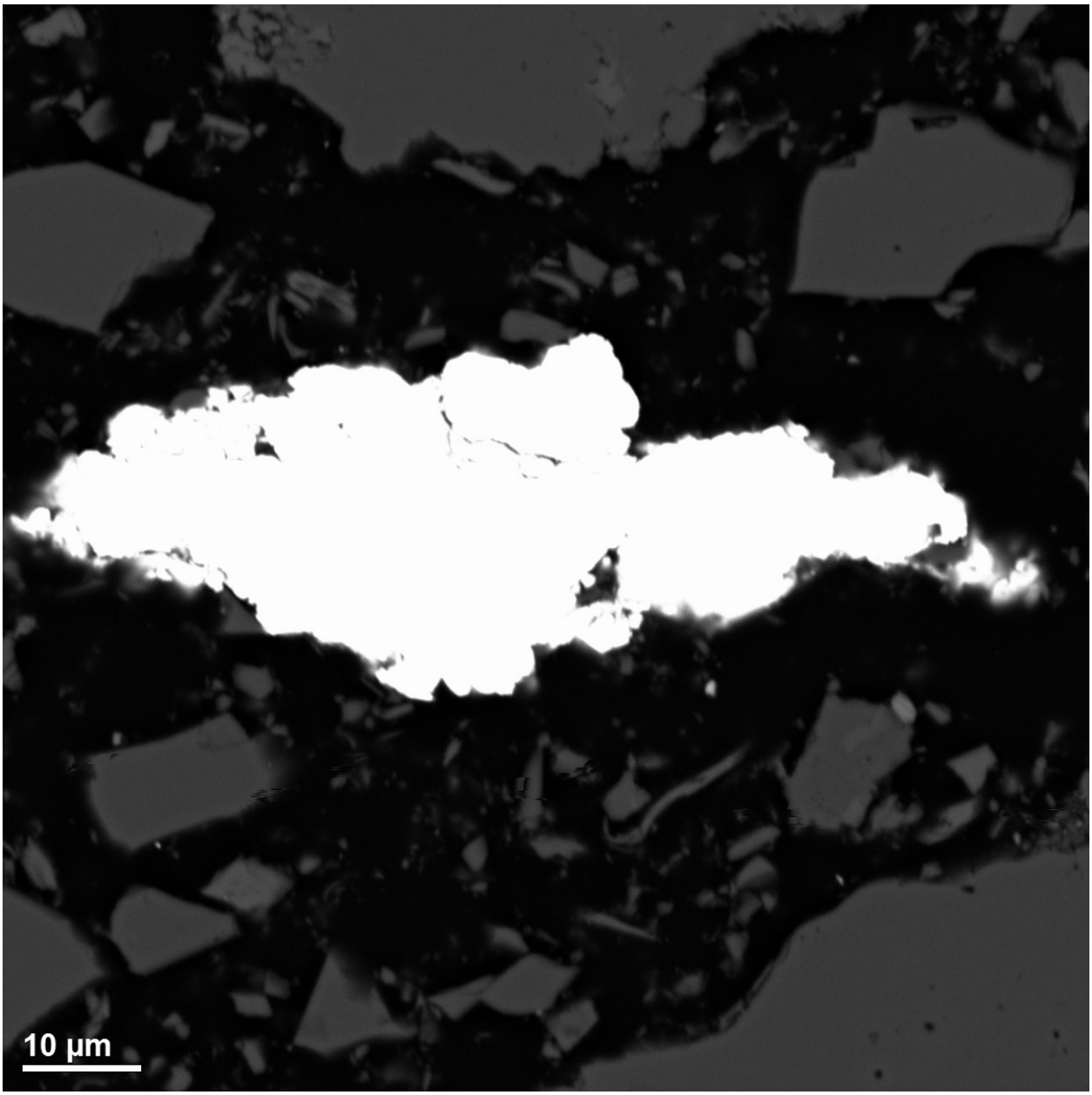

Figure 8: Irregular Grain of Electrum. The Composition, on an Atomic Basis, is Approximately $Au_{80}Ag_{20}$.

Monazite, zircon, and xenotime occurred as very fine grains, in trace amounts.

Additional backscattered electron images are provided in the Appendix.

LGV Rhyolite Pulp Sample

The sample consisted of discrete grain fragments and lesser amounts of lithic fragments (mostly <100 µm, but rarely 100 µm – 500 µm) as depicted by Figure 9. The abundance of lithic fragments was higher than in the HGV Rhyolite Pulp Sample. Lithic fragments generally consisted of quartz, K-feldspar, and albite in varied proportions.

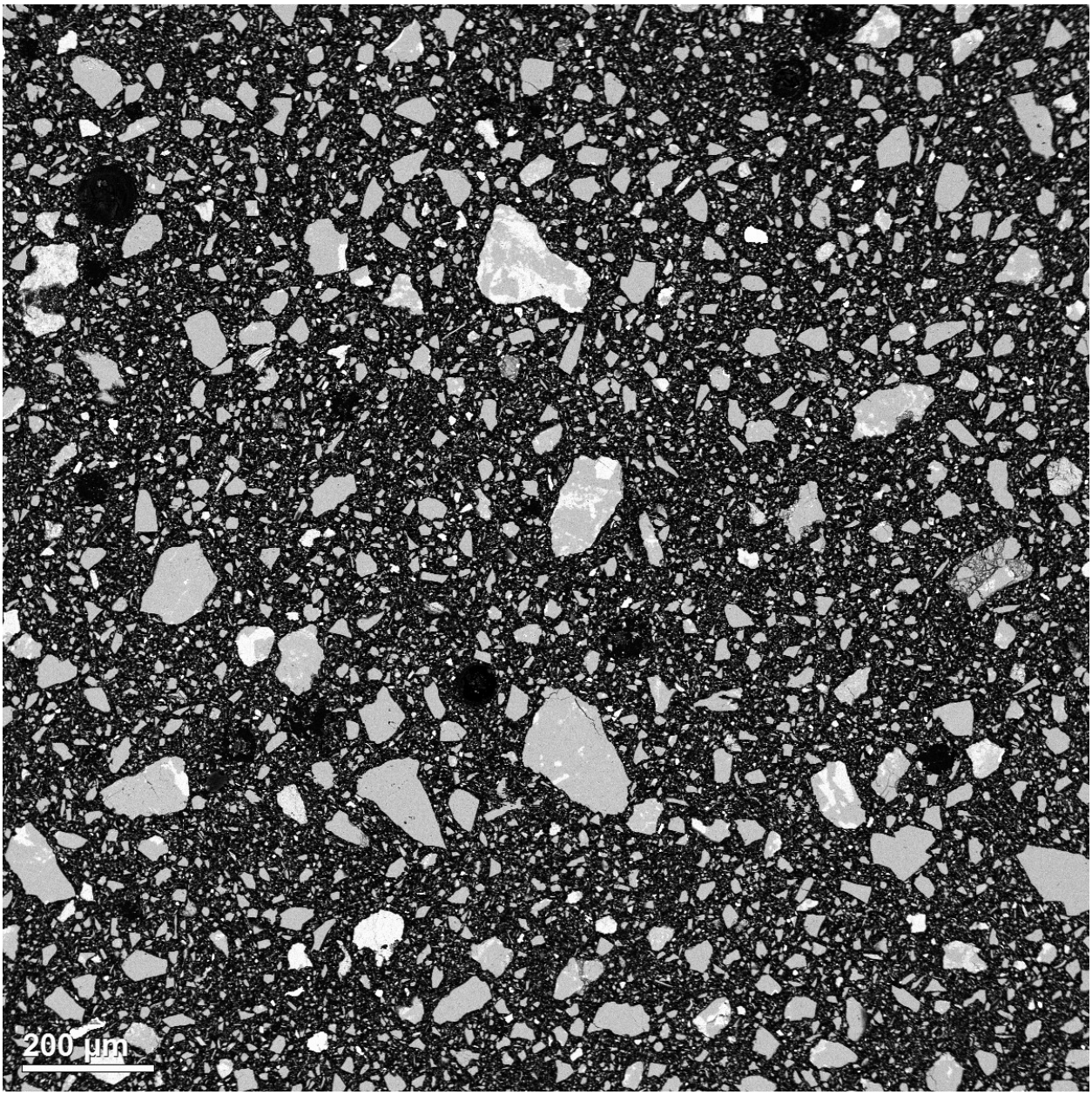

Figure 9: Low Magnification Overview.

Quartz was most abundant and tended to be coarser-grained than feldspar. K-feldspar most commonly occurred as an interstitial phase. However, K-feldspar tended to be coarser and more abundant in albite-rich fragments (see Figure 10). Rutile, muscovite, and Fe-carbonate may also be present. Monazite and zircon were less commonly observed.

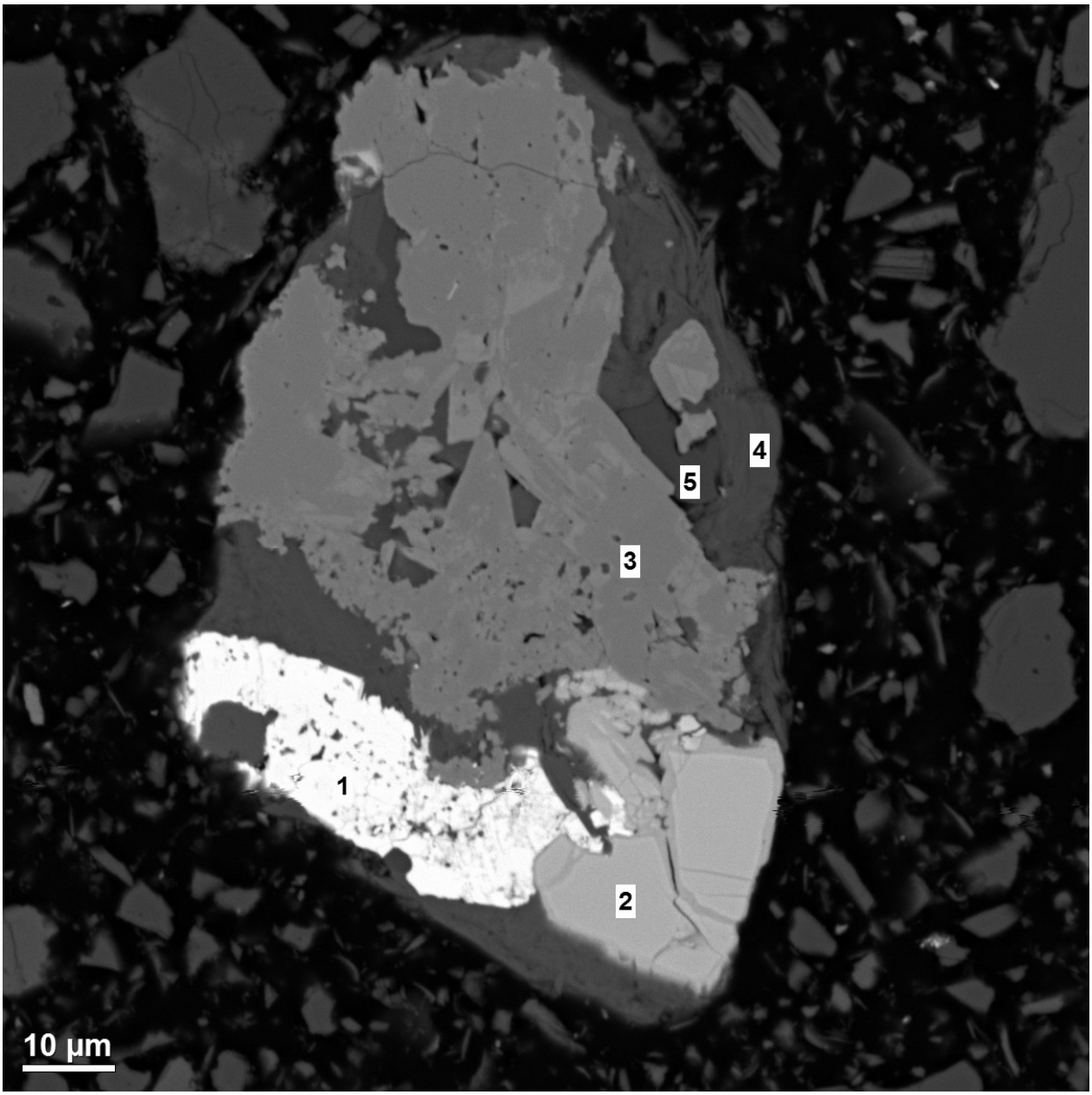

Figure 10: Fragment Consisting of 1) Monazite, 2) Zircon, 3) Rutile, 4) Muscovite, and 5) Albite. The Brighter Areas in the Rutile are Enriched in Tungsten and Niobium.

Quartz was the most abundant discrete mineral fragment, followed by albite. Discrete grains of K-feldspar were rare (see Figure 11). Muscovite, rutile, monazite, and zircon also occurred as uncommon discrete grains (<50 µm). Fe-hydroxide also occurred as discrete, inhomogeneous grain fragments, with varied minor contents of Al, Si, K, and Mn.

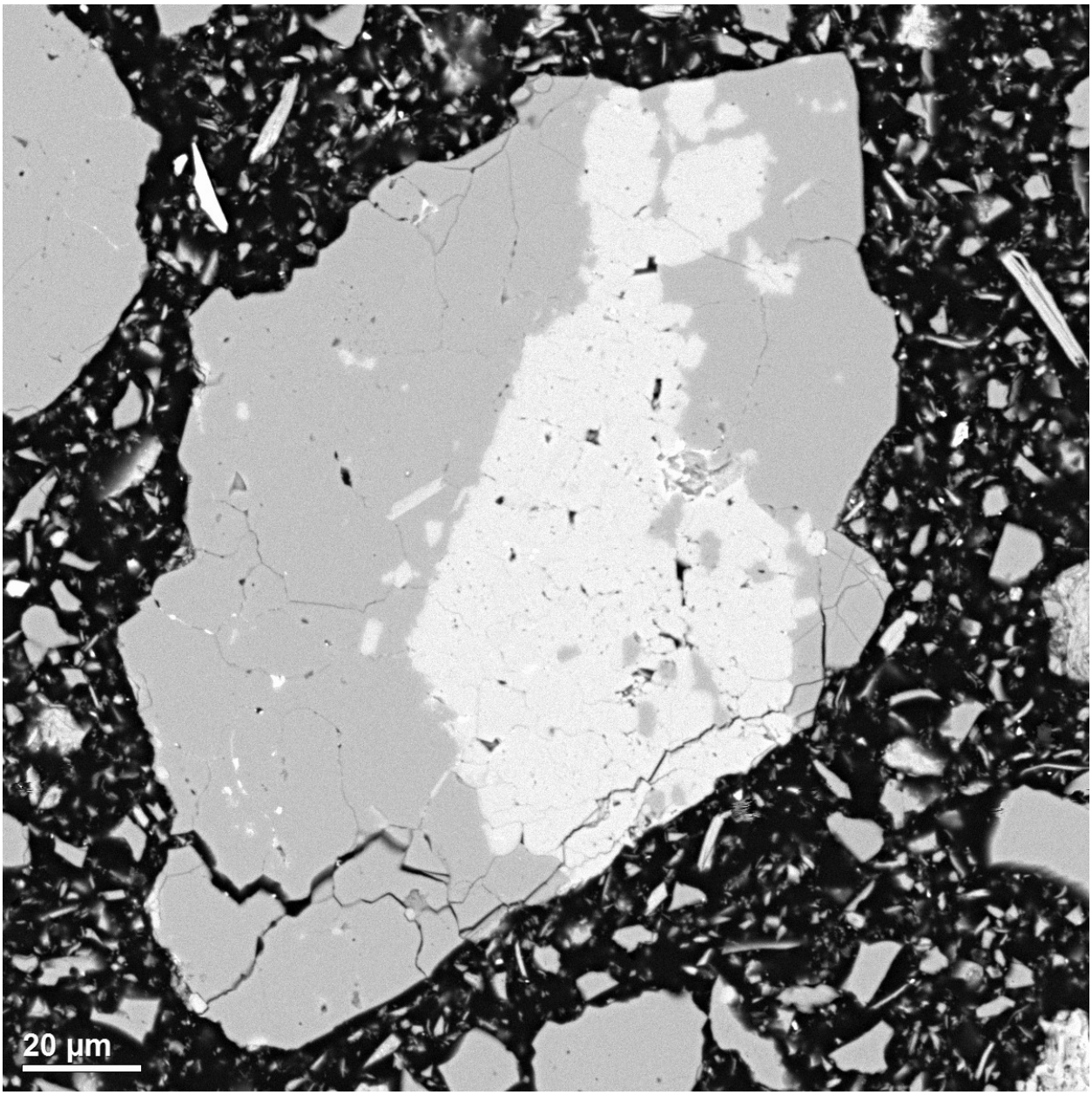

Figure 11: Fragment Consisting of K-Feldspar (Light Grey) and Quartz (Medium Grey). The Quartz Contains Small Elongate Inclusions of Muscovite (Light Grey).

Sulphide minerals were virtually absent. One discrete grain of pyrite was observed.

Additional backscattered electron images are provided in the Appendix.

Cyanide Leaching Characterization

A representative sub-sample each of the HGV Rhyolite Pulp Sample, LGV Rhyolite Pulp Sample, and LGV Rhyolite Rejects Combined Gravity Concentration material was prepared for cyanide leaching characterization test work. Bottle roll cyanidation tests were conducted to evaluate the leachability properties of each sample. The operating conditions and results are detailed in Table 5 and Table 6. Bottle rolls were conducted at

50% solids for both pulp samples (HGV Rhyolite and LGV Rhyolite), and 40% for the combined gravity concentration sample (LGV Rhyolite Rejects), with the two pulp samples (HGV Rhyolite and LGV Rhyolite) utilizing a NaCN concentration of 2 g/L and the combined gravity concentrate on LGV Rhyolite Rejects utilizing 10 g/L.

Table 5
Bottle Roll Testing Operating Conditions and Solids Assays

TEST ID	Leachate pH			Cons. (kg/t)		Meas. Head Grade	Calc. Head Grade	Residue Grade (%)
	Initial	Start	Final	CaO	NaCN	Au (g/t)	Au (g/t)	Au (g/t)
HGV Pulp	6.3	11.2	11.3	3.31	0.53	29.58	32.81	0.10
LGV Pulp	7.1	11.2	11.3	3.54	0.19	0.79	0.37	0.00
LGV Gravity Conc	6.8	11.9	11.8	3.54	1.98	17.35	18.07	0.01

Table 6
Results from CN Bottle Roll Testing

TEST ID	Au Extracted (mg/L)					Au Extracted (mg/kg)					Au Extracted (%)				
Time (hr.):	1.0	2.5	6.0	24.0	48.0	1.0	2.5	6.0	24.0	48.0	1.0	2.5	6.0	24.0	48.0
HGV Pulp	12.8	19.8	27.20	32.30	32.50	12.88	19.93	27.38	32.51	32.71	39.3	60.7	83.4	99.1	99.7
LGV Pulp	0.17	0.28	0.35	0.37	0.37	0.17	0.28	0.35	0.37	0.37	45.3	74.7	93.4	98.7	98.7
LGV Gravity. Conc	2.75	4.90	8.67	13.55	13.43	4.13	7.16	12.12	18.06	17.92	22.9	39.6	67.1	100.0	99.2

Table 6 indicated that all three samples were amenable to cyanidation with Au extractions obtained ranging from 98.7 % to 99.7 % with NaCN consumption ranging from 0.19 kg/t to 1.98 kg/t.

CONCLUSIONS AND RECOMMENDATIONS

Note that all results were only as representative as the sample received. The material did display a nugget effect with some variances between calculated and measured head grades observed especially for the LGV Rhyolite Rejects material. Data obtained showed that:

- Approximately 9 kg each of the HGV Rhyolite Pulp, LGV Rhyolite Pulp and LGV Rhyolite Rejects samples were received and prepared for the scoping study and measured head grades of 28.83 g/t Au, 0.43 g/t Au and 0.46 g/t Au respectively were obtained.
- Based on the results obtained during the study, the Rhyolite material tested was amenable to cyanidation with Au extraction values of 99.7 % and 98.7 % obtained on the Pulp samples and 99.2 % Au extraction obtained on a centrifugal gravity concentrate blend from the LGV Rhyolite Rejects.
- Centrifugal gravity concentration test work on the LGV Rhyolite Rejects material at a grind size of 100 % passing 1.0 mm resulted in 92.0 % Au distribution to the concentrate fraction in 3.9 % of the mass to obtain a grade of 35.00 g/t Au. It was noted that the calculated head grade in this test was 1.49 g/t Au compared to the 0.46 g/t Au measured value and a nugget effect is present. Further test work on a larger sample is recommended to confirm the representivity of these results.
- Through mineralogical analyses it was seen that the Rhyolite material comprised largely of quartz, albite and K-Feldspar and the clay-mineral, muscovite, was present. One grain of electrum was seen in the HGV Rhyolite Pulp sample, and it had an atomic composition of $Au_{80}Ag_{20}$.
- Size-by-assay analyses of the LGV Rhyolite Rejects sample indicated a tendency of the Au to upgrade to the fines fraction.
- Larger scale testing is recommended to investigate scale-up factors and the presence of Au nuggets. Further analyses could include different zones from the Williams Brook gold deposit.
- Further test work on a larger sample to increase the representativity of the deposit is recommended as well as variability test work. This test work should include confirming the optimal liberation size required in order to beneficiate the gold from the deposit.
- It is recommended that alternative and additional extraction methods such as Dense Media Separation, ore sorting, and flotation be evaluated.
- Cyanidation optimization test work is recommended on the larger sample to confirm optimal operating conditions such as retention time, NaCN concentration etc. in order to define a preliminary flow sheet.

APPENDIX

Sample Received and Prepared

Table 7
HGV Rhyolite Pulp Sample Blending Ratio

DDH	Sample	Pulp Mass (g)	From (m)	To (m)	Sample Length	Lithology	Sample ALS	Au-Best	Report
WB21-02	C733683	657.4	7.2	8.1	0.9	Rhyolite	C733683	9.290	MN21187151
WB21-02	C733684	657.2	8.1	9	0.9	Rhyolite	C733684	0.029	MN21187151
WB21-02	C733691	701.4	13.7	14.2	0.5	Rhyolite	C733691	18.800	MN21187151
WB21-02	C733692	410.4	14.2	14.5	0.3	Quartz Vein	C733692	80.000	MN21187151
WB21-02	C733693	518.4	14.5	15	0.5	Rhyolite	C733693	0.065	MN21187151
WB21-02	C733694	818.3	15	15.5	0.5	Rhyolite	C733694	0.052	MN21187151
WB21-02	C733695	460.3	15.5	15.8	0.3	Rhyolite	C733695	88.100	MN21187151
WB21-02	C733739	913.0	45.6	46.1	0.5	Quartz Vein	C733739	23.300	MN21187151
WB21-02	C733740	624.0	46.1	46.6	0.5	Quartz Vein	C733740	116.500	MN21187151
WB21-02	C733743	840.6	47.59	48.2	0.61	Quartz Vein	C733743	38.600	MN21187151
WB21-02	C733744	757.6	48.2	48.85	0.65	Quartz Vein	C733744	72.000	MN21187151
WB21-02	C733745	688.9	48.85	49.45	0.6	Quartz Vein	C733745	67.400	MN21187151
WB21-05	C730182	745.9	26	26.9	0.9	Rhyolite	C730182	8.450	MN21201555
WB21-05	C730183	841.7	26.9	27.5	0.6	Quartz Vein Stw	C730183	13.500	MN21201555
WB21-05	C730184	735.8	27.5	28	0.5	Quartz Vein Stw	C730184	19.150	MN21201555
WB21-12	D278218	654.3	53	54	1	Rhyolite	D278218	8.540	MN21230588

Table 8
LGV Rhyolite Pulp Sample Blending Ratio

DDH	Sample	Pulp Mass (g)	From (m)	To (m)	Sample Length	Lithology	Sample ALS	Au-Best	Report
WB21-02	C733705	815.0	20	21	1	Rhyolite	C733705	0.262	MN21187151
WB21-02	C733706	705.3	21	22	1	Rhyolite	C733706	2.890	MN21187151
WB21-03	C733871	961.2	21.65	22.45	0.8	Rhyolite	C733871	0.161	MN21194497
WB21-02	C733727	808.2	36.2	37	0.8	Rhyolite	C733727	0.504	MN21187151
WB21-02	C733728	361.9	37	37.4	0.4	Rhyolite	C733728	0.333	MN21187151
WB21-03	C733940	788.6	71.2	71.8	0.6	Quartz Vein	C733940	0.157	MN21194497
WB21-03	C733942	815.3	72.55	73.1	0.55	Quartz Vein	C733942	0.674	MN21194497
WB21-03	C733943	988.2	73.1	73.75	0.65	Quartz Vein	C733943	0.336	MN21194497
WB21-04	C730054	675.9	87.3	88	0.7	Rhyolite	C730054	0.167	MN21195394
WB21-05	C730197	848.8	37.8	38.4	0.6	Rhyolite	C730197	0.711	MN21201555
WB21-14	D278634	662.1	116	117	1	Rhyolite	D278634	0.156	MN21239140
WB21-16	D278936	1014.3	95	96	1	Rhyolite	D278936	0.675	MN21234763

Table 9
LGV Rhyolite Reject Sample Blending Ratio

DDH	Sample	Reject Mass (g)	From (m)	To (m)	Sample Length	Lithology	Sample ALS	Au-Best	Report
WB21-02	C733706	963.6	21	22	1	Rhyolite	C733706	2.890	MN21187151
WB21-02	C733730	636.9	38.4	39.4	1	Rhyolite	C733730	0.215	MN21187151
WB21-07	C734026	405.9	32	33	1	Rhyolite	C734026	1.220	MN21214648
WB21-07	C734027	674.0	33	34	1	Rhyolite	C734027	0.228	MN21214648
WB21-08	C734341	621.8	26.9	27.9	1	Quartz vein	C734341	0.747	MN21221714
WB21-09	C733432	994.4	49	50	1	Rhyolite	C733432	0.141	MN21221963
WB21-09	C733433	1143.6	50	51	1	Rhyolite	C733433	0.122	MN21221963
WB21-13	D278369	356.2	29.4	30.15	0.75	Quartz vein zone	D278369	0.191	MN21230588

Particle Size Distribution (PSD) Results

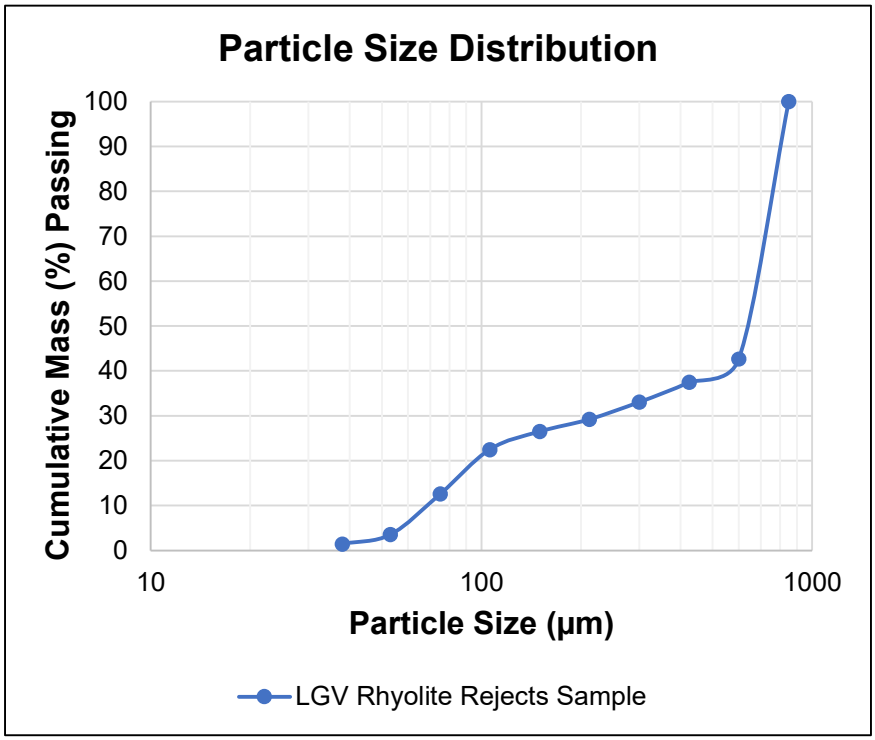

Figure 12: Particle Size Distribution.

Backscattered Electron Images on HGV Rhyolite Pulp Sample

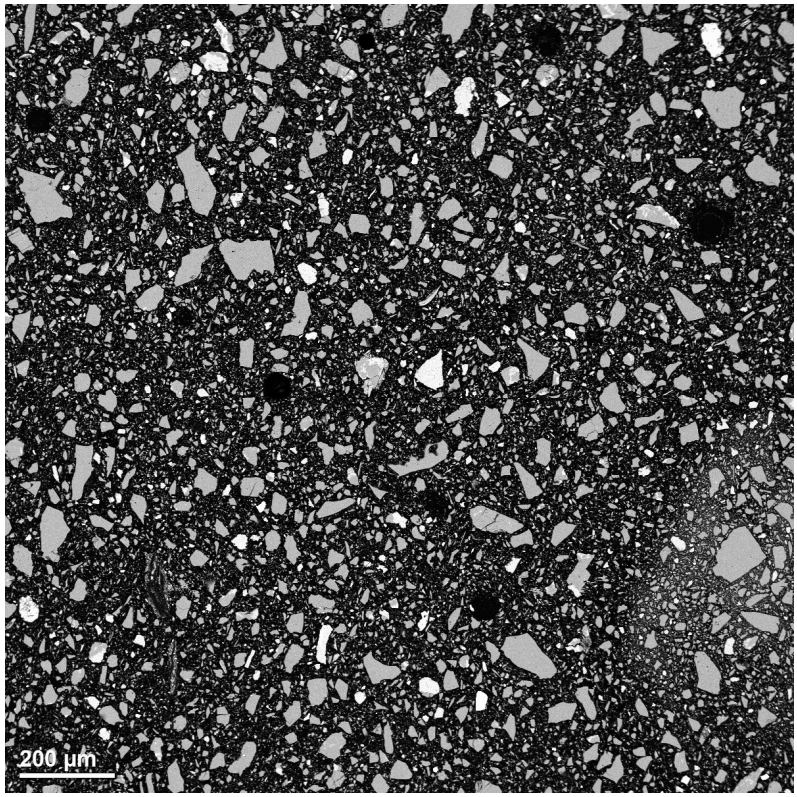

Figure 13: Low Magnification Overview.

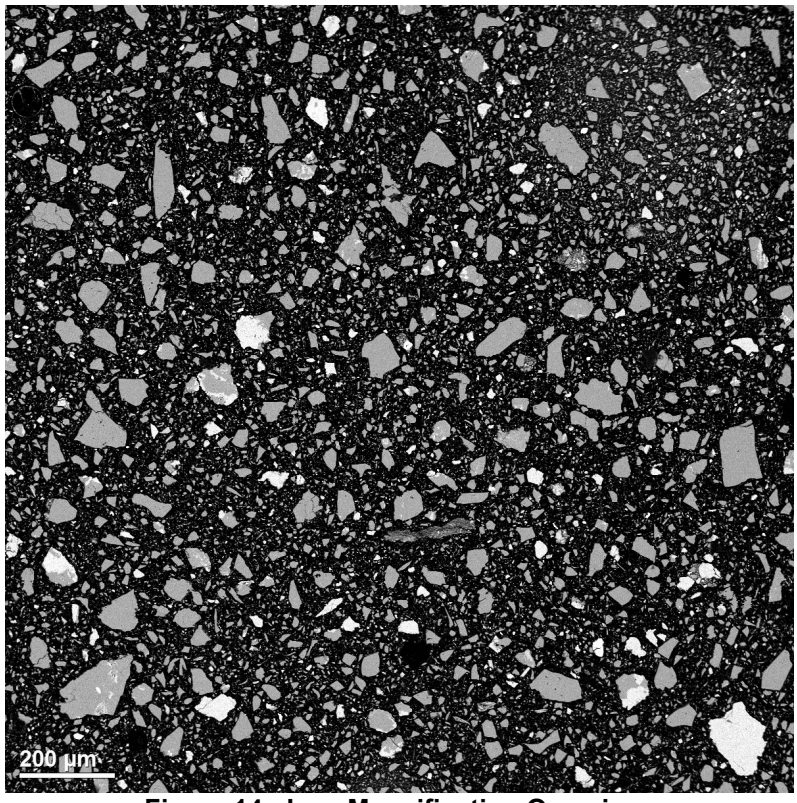

Figure 14: Low Magnification Overview.

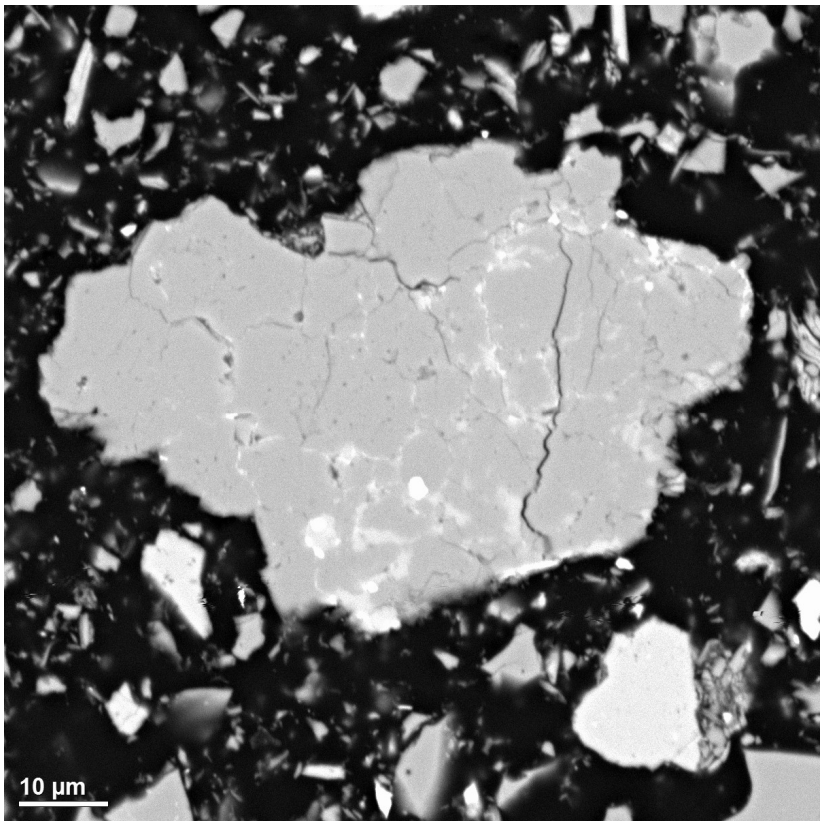

Figure 15: Irregular Fragment of Albite (Medium Grey), with Fine Inclusions of K-Feldspar (Light Grey). Brighter Grain at Bottom Right is K-Feldspar.

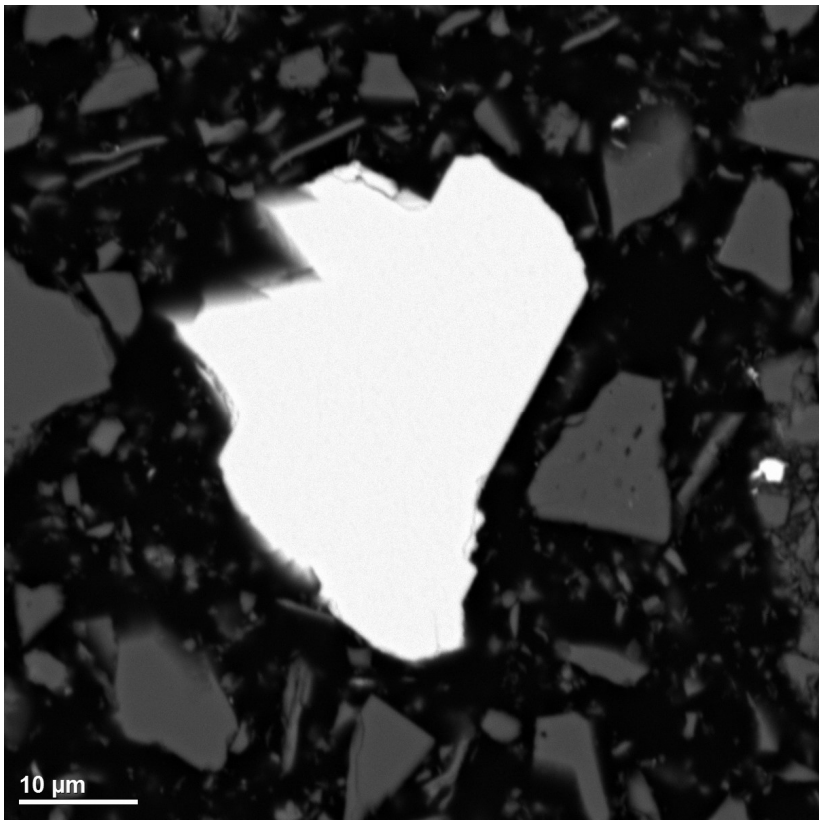

Figure 16: Discrete, Angular Fragment of Sphalerite.

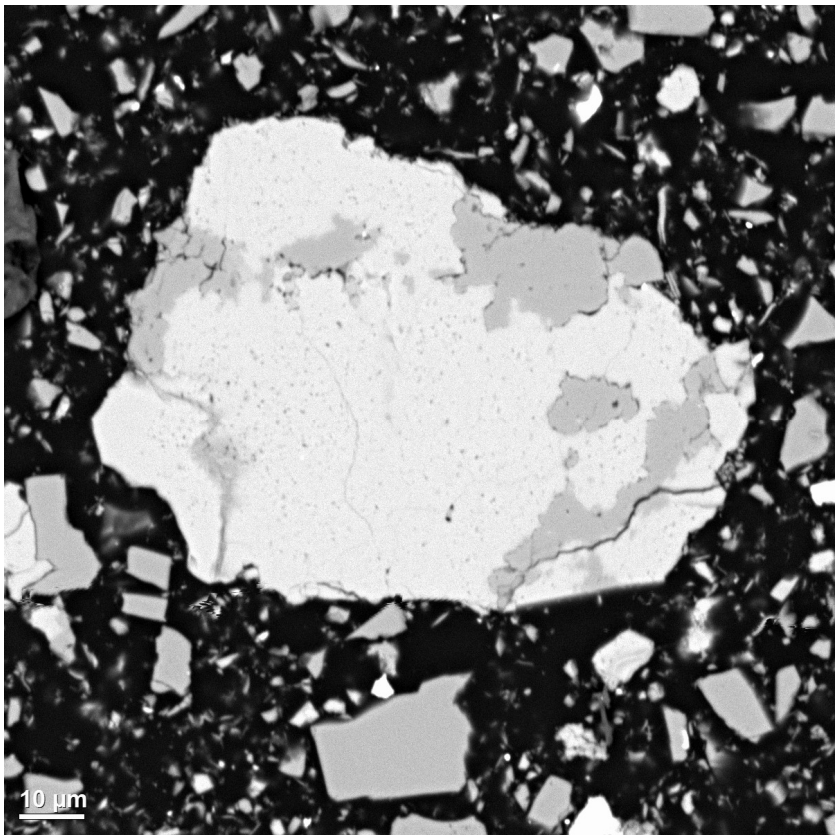

Figure 17: Fragment Consisting of K-Feldspar (Light Grey) and Albite (Medium Grey).

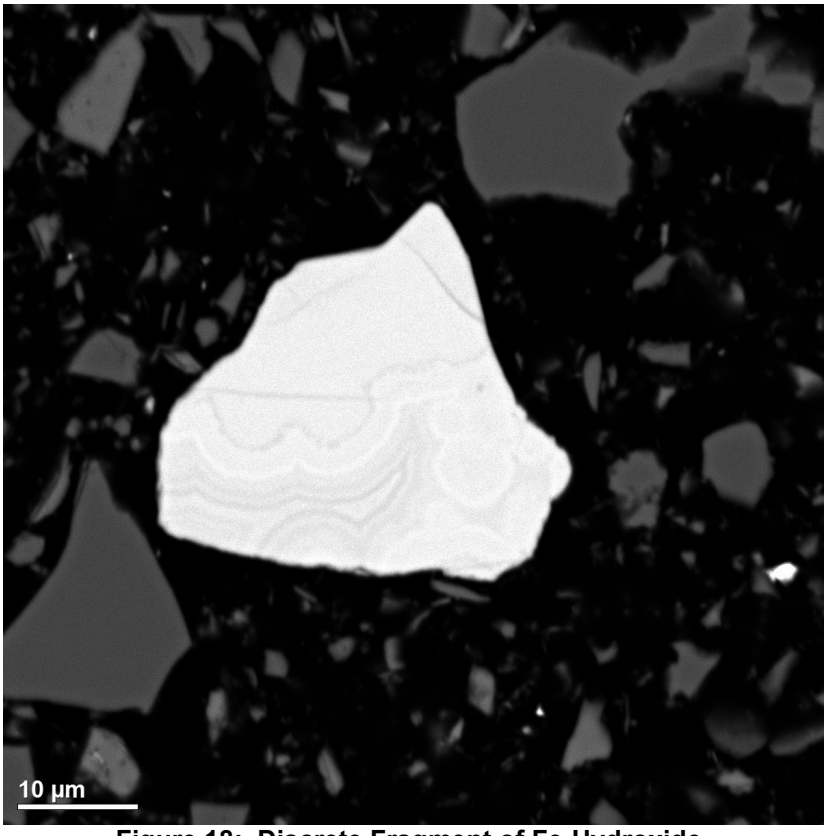

Figure 18: Discrete Fragment of Fe-Hydroxide.

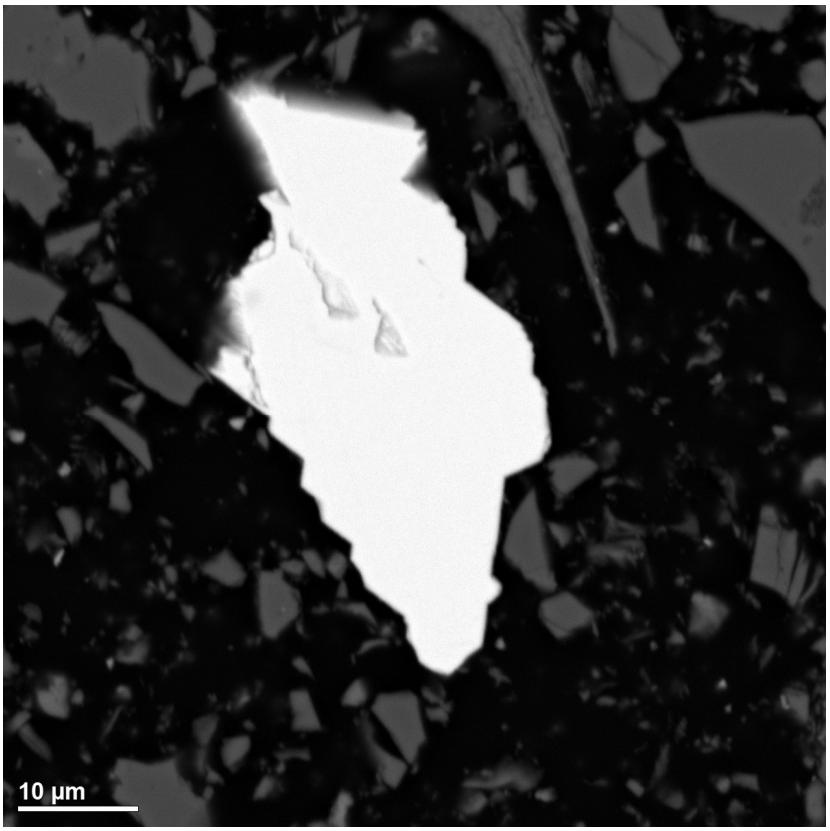

Figure 19: Discrete, Angular Fragment of Sphalerite.

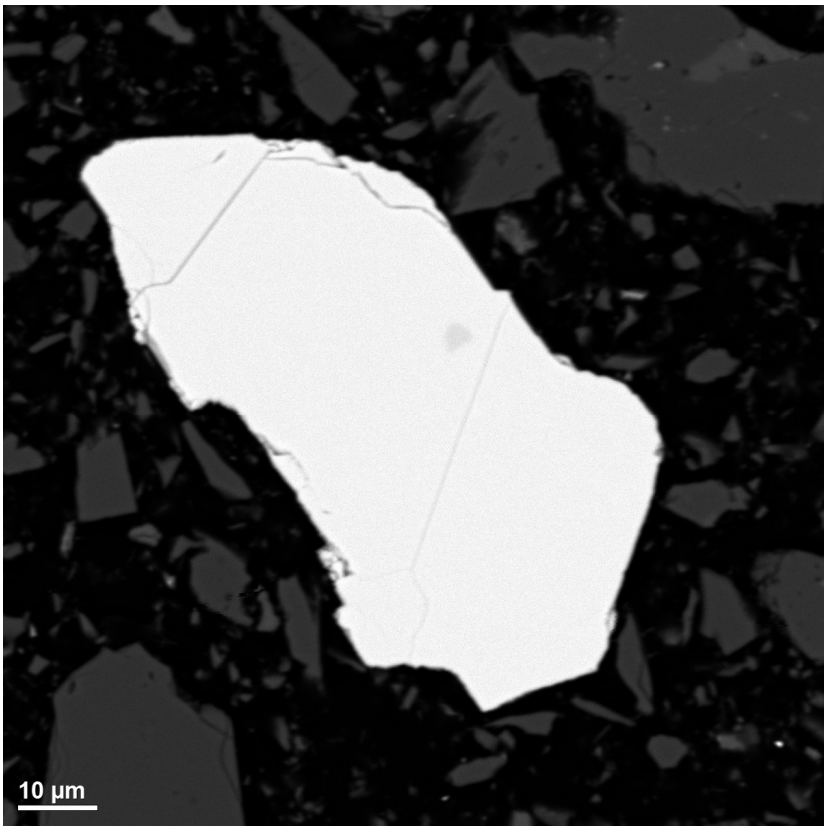

Figure 20: Discrete Fragment of Sphalerite. Small Darker Grains of Chalcopyrite are Included.

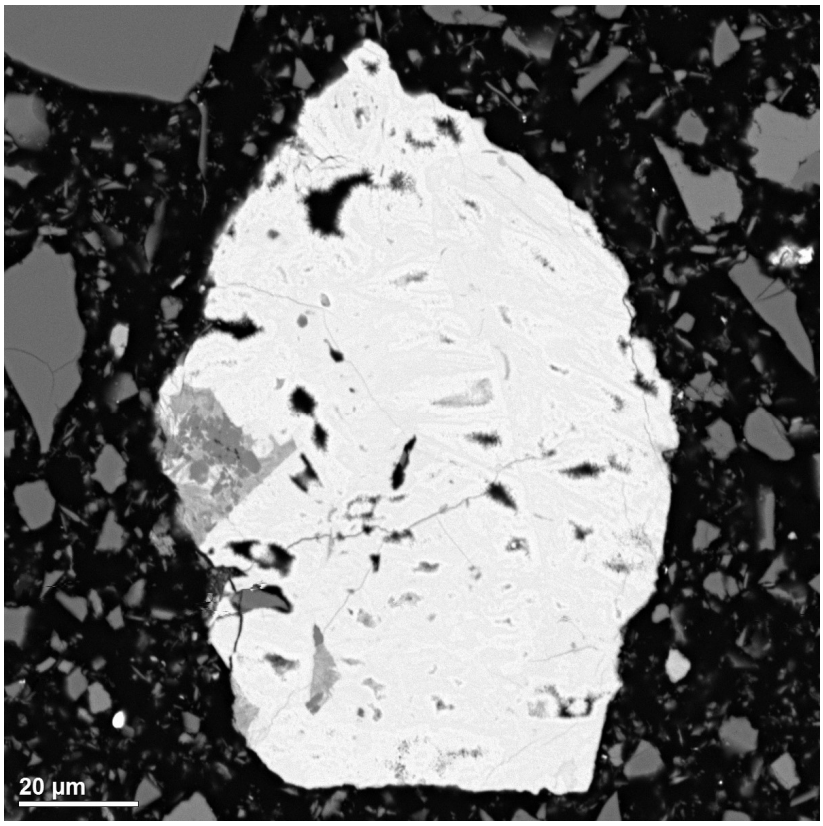

Figure 21: Fragment of Fe-Hydroxide.

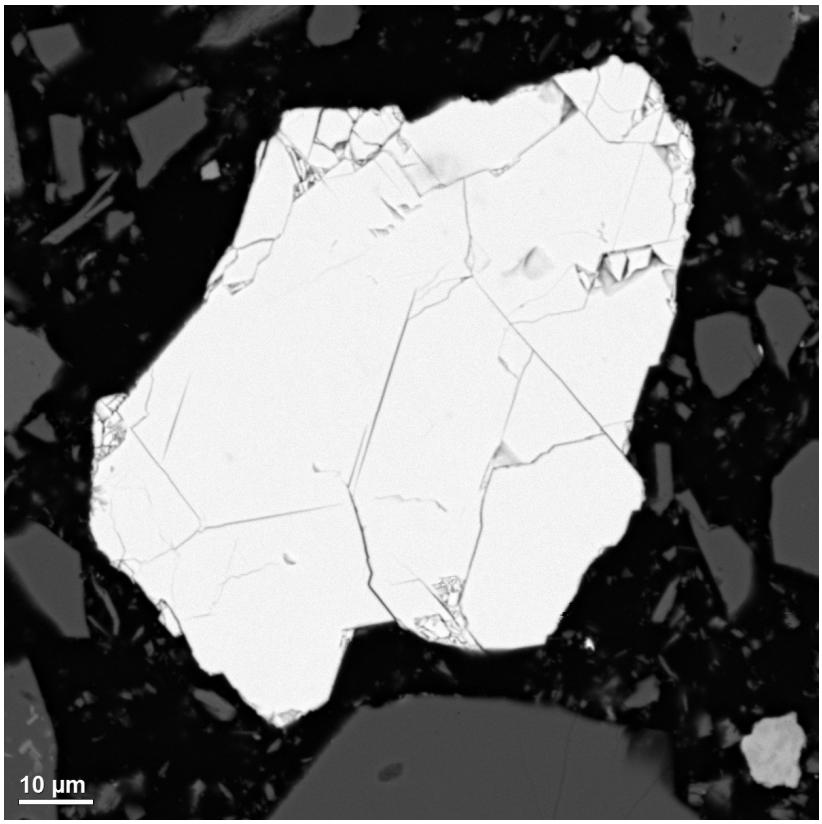

Figure 22: Discrete Fragment of Sphalerite, with a Small Grain of Fe-Hydroxide at Bottom-Right of Image.

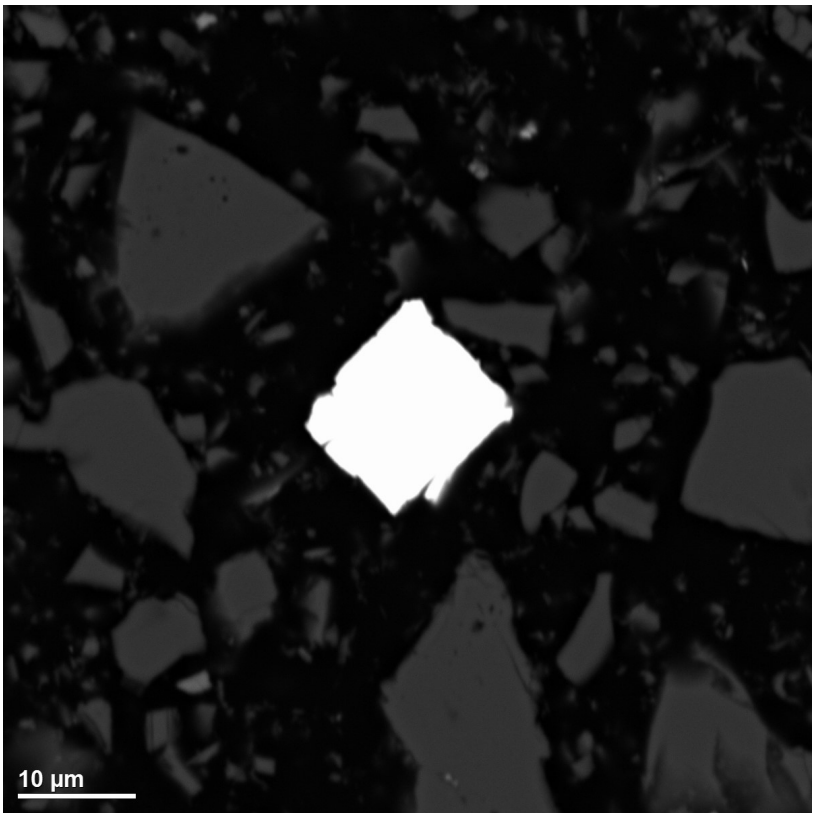

Figure 23: Small Euhedral Grain of Galena.

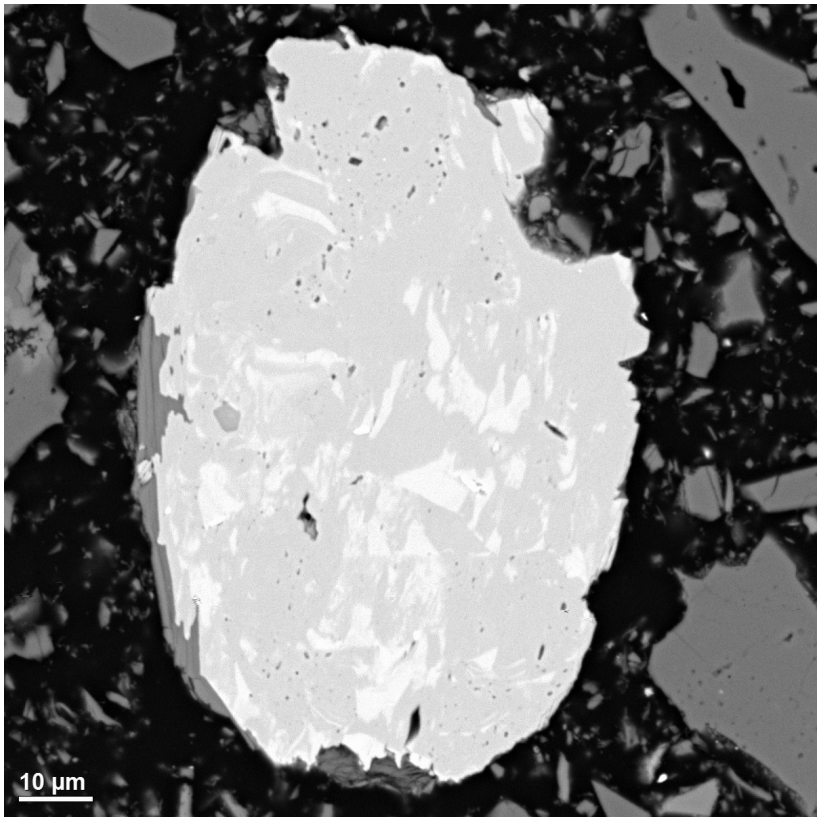

Figure 24: Oval Fragment of Rutile. Bright Areas are Enriched in Tungsten and Niobium. A Grain of Muscovite Occurs Along the Left Edge (Medium Grey).

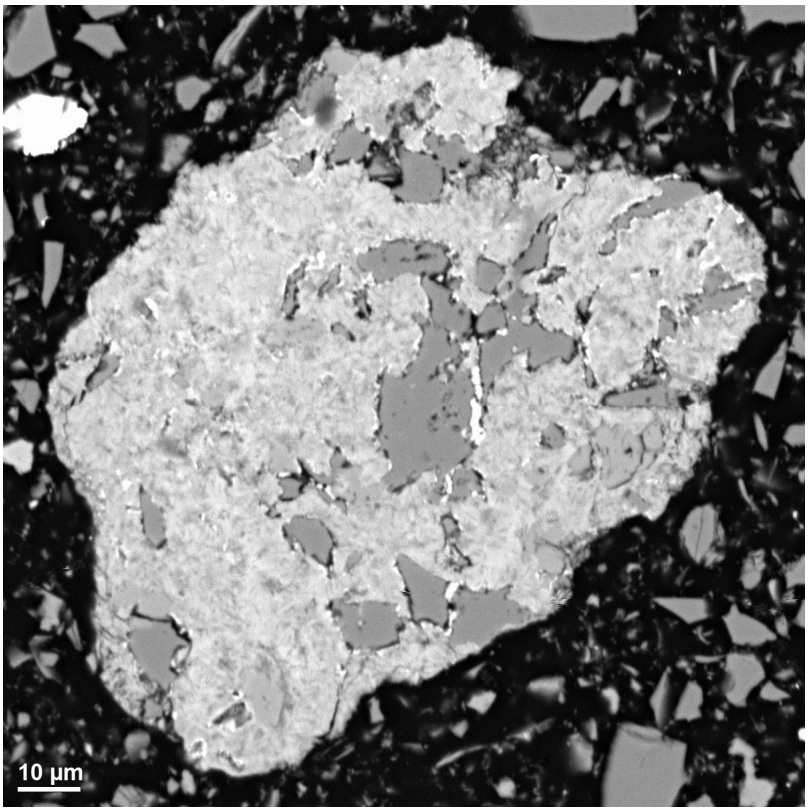

Figure 25: Fragment Consisting of Fine-Grained Chlorite (Light Grey), with Inclusions of Albite (Medium Grey).

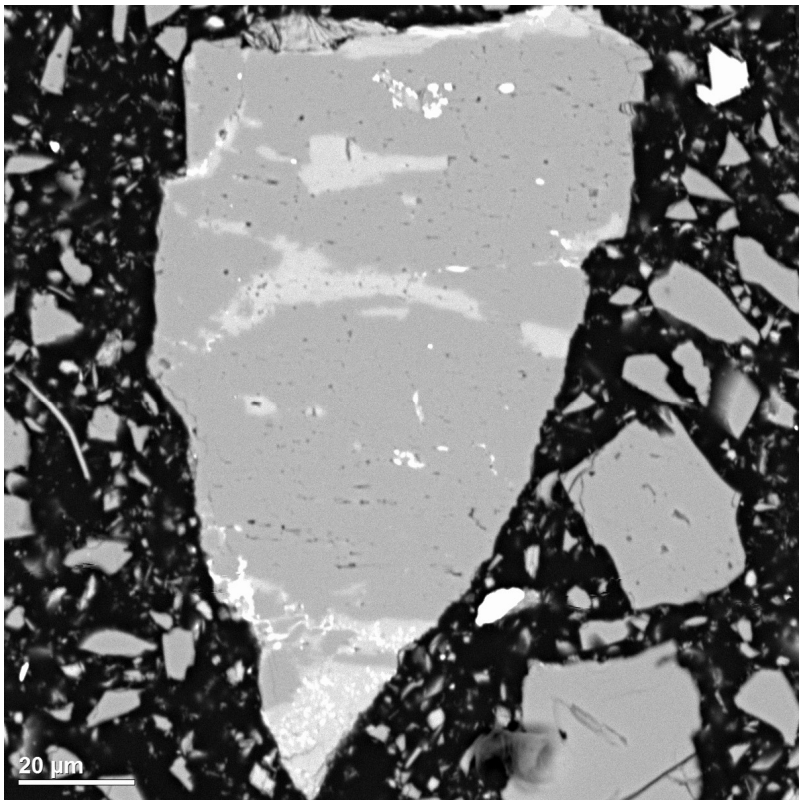

Figure 26: Fragment of Albite (Medium Grey) and K-Feldspar (Light Grey), with Minor Fine-Grained Fe-Oxide (White). Bright Fine Grain at Top-Right of Image is Fe (Mg)-Carbonate.

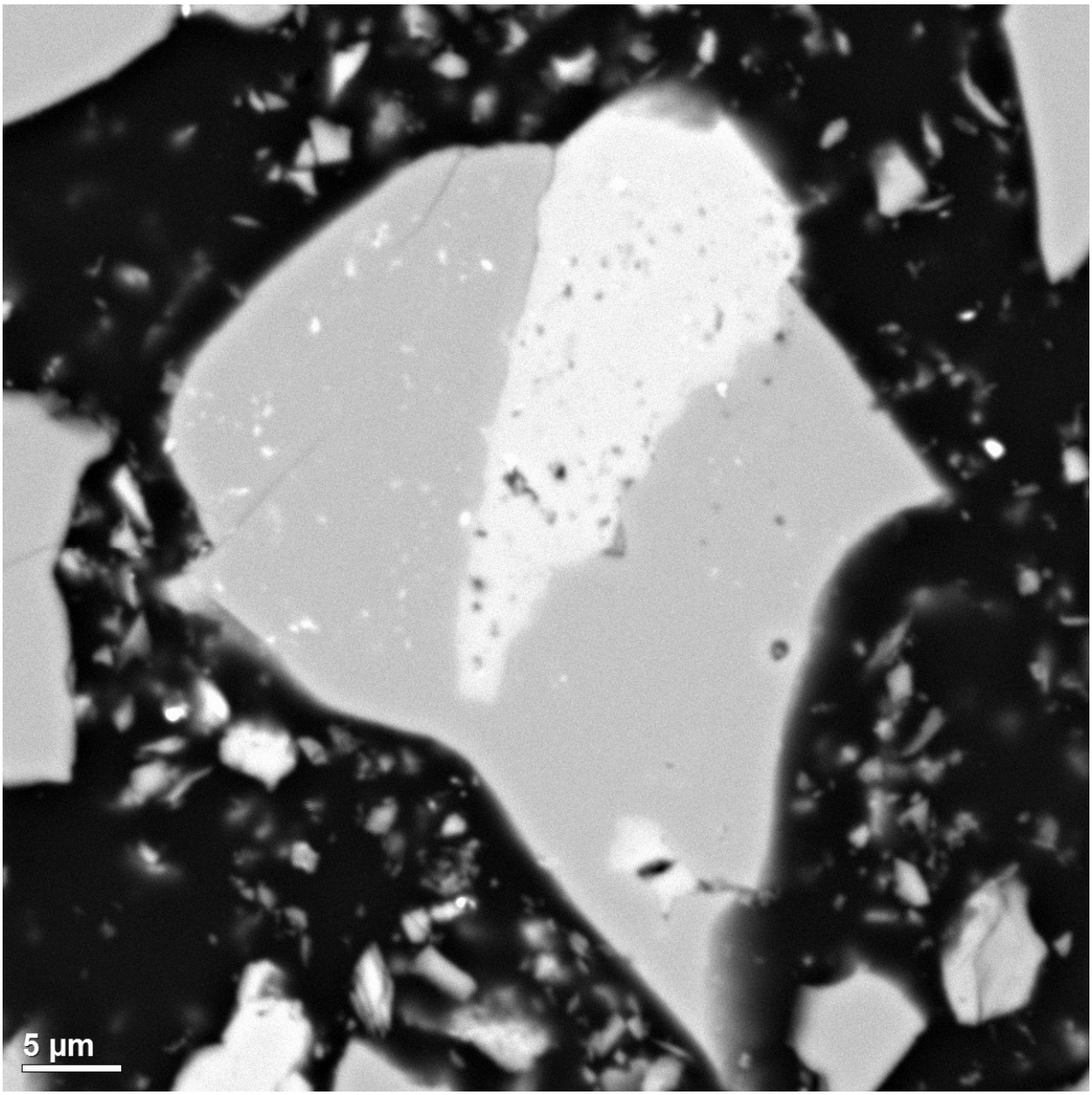

Figure 27: Fragment Consisting of K-Feldspar (Light Grey) and Quartz (Medium Grey).

Backscattered Electron Images on LGV Rhyolite Rejects Combined Gravity Concentrate

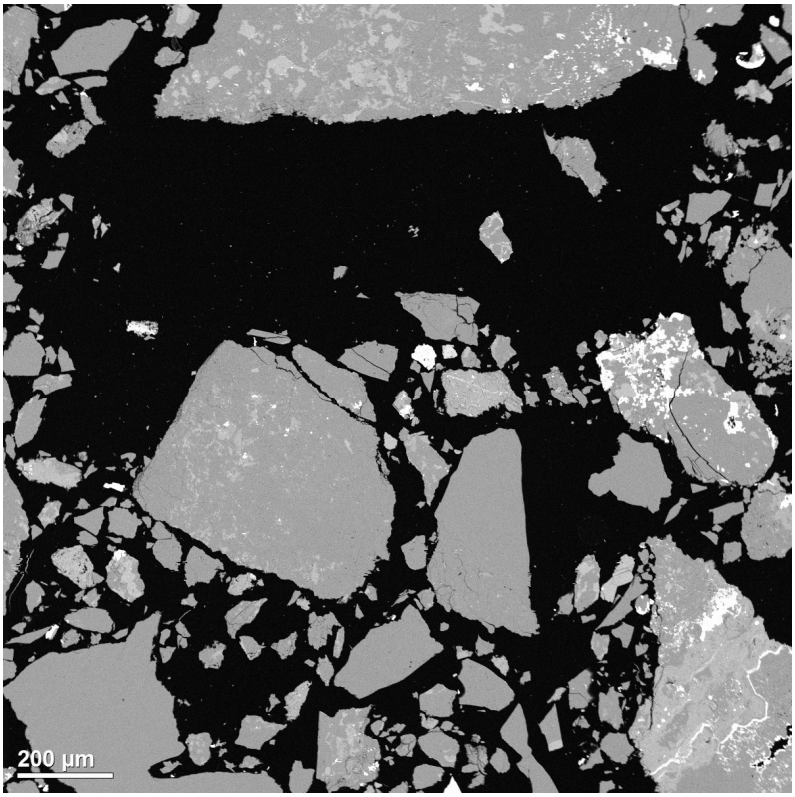

Figure 28: Low Magnification Overview.

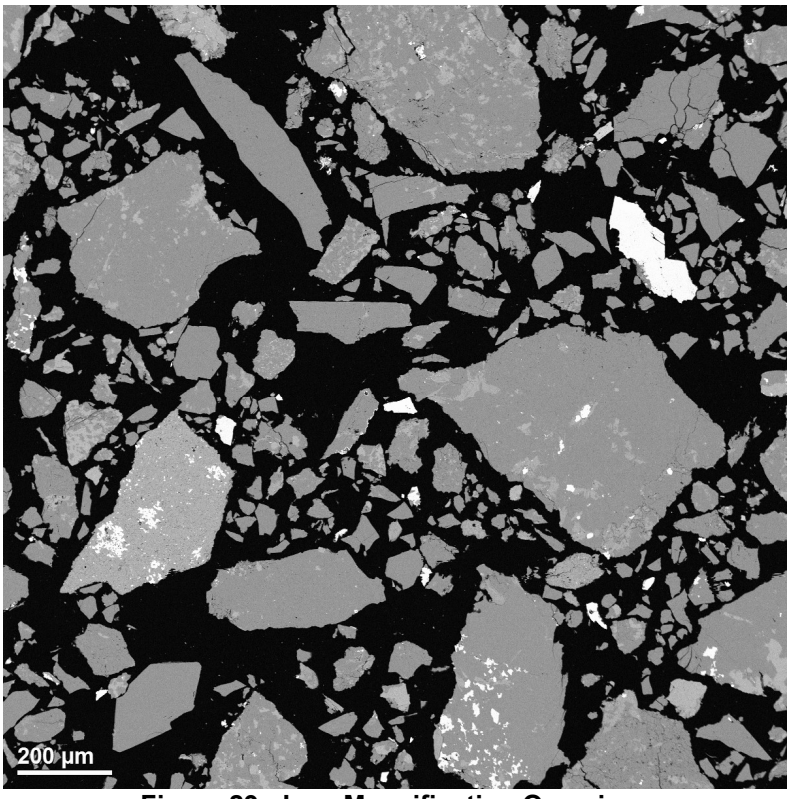

Figure 29: Low Magnification Overview.

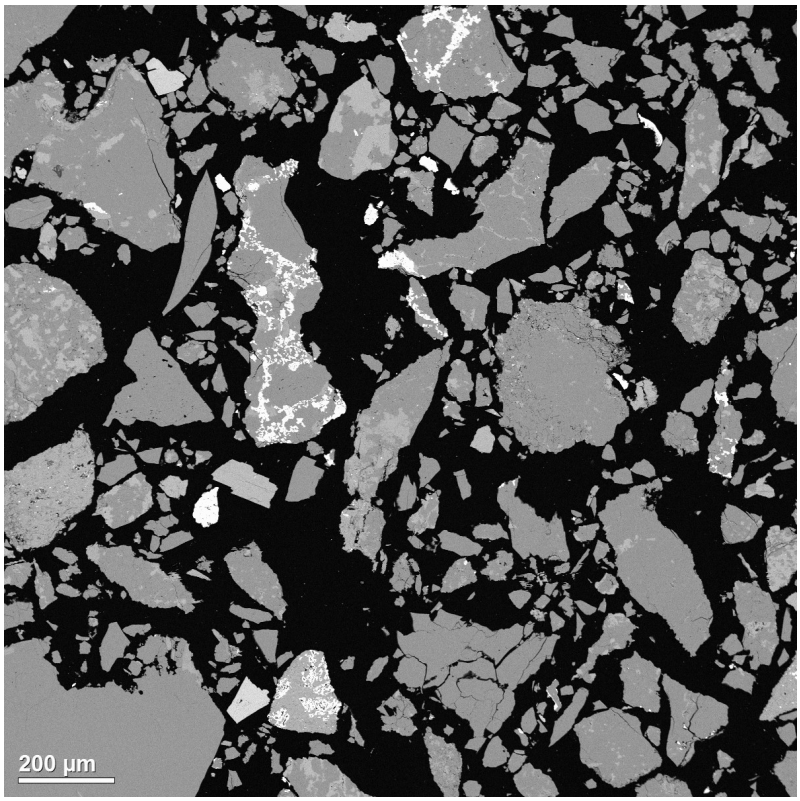

Figure 30: Low Magnification Overview.

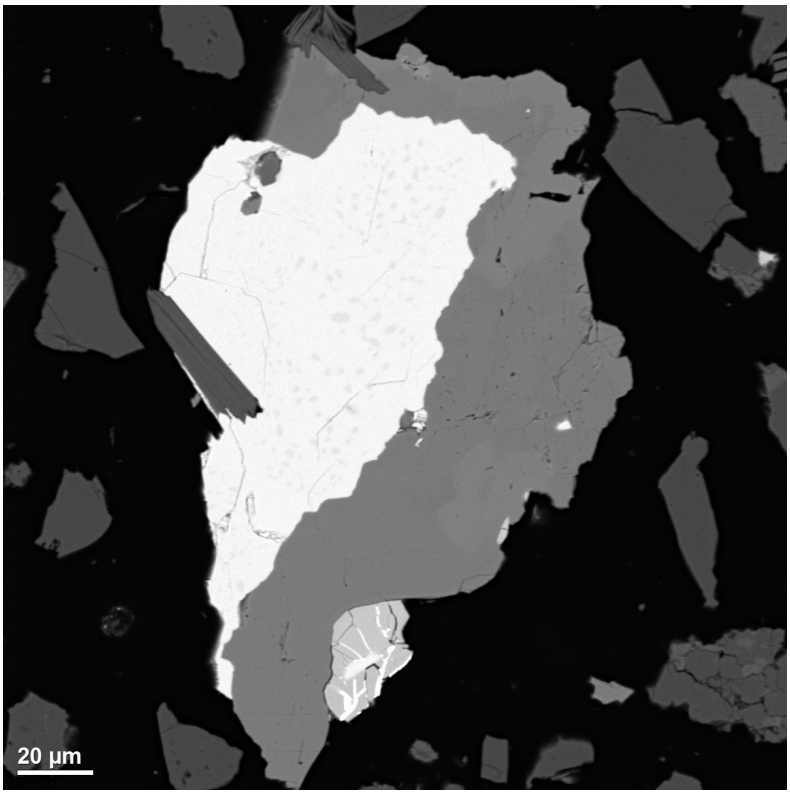

Figure 31: Fragment Consisting of Sphalerite (Light Grey), Fe-Carbonate (Dark Grey), and Pyrite (Medium Grey; Bottom). Sphalerite has Fine-Grained Darker Inclusions of Chalcopyrite. The Pyrite Contains Inclusions of Sphalerite as well as Thin Veinlets of Galena.

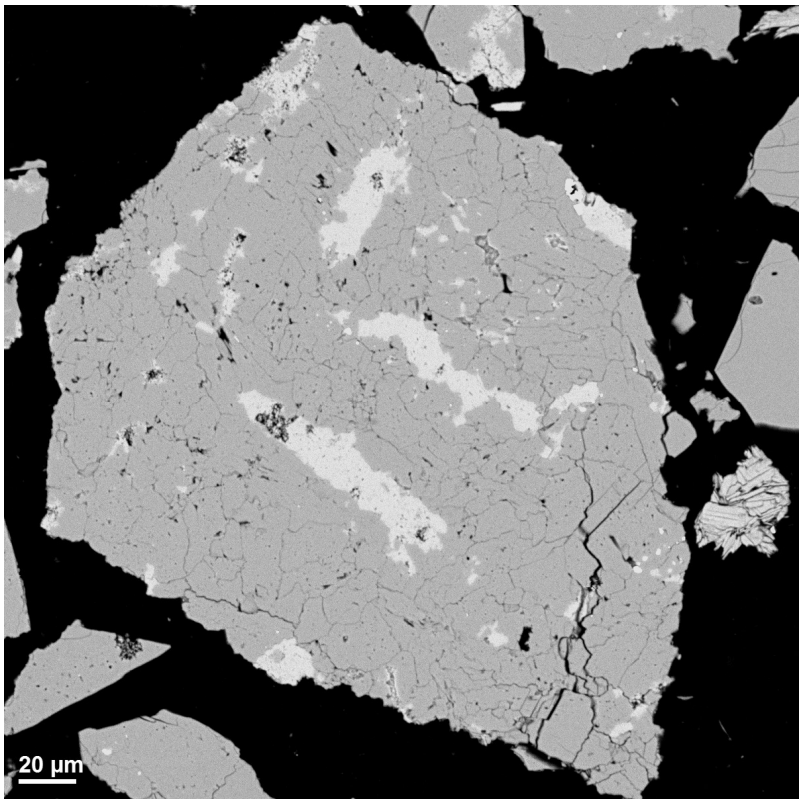

Figure 32: Fragment Consisting of K-Feldspar (Light Grey) and Albite (Medium Grey).

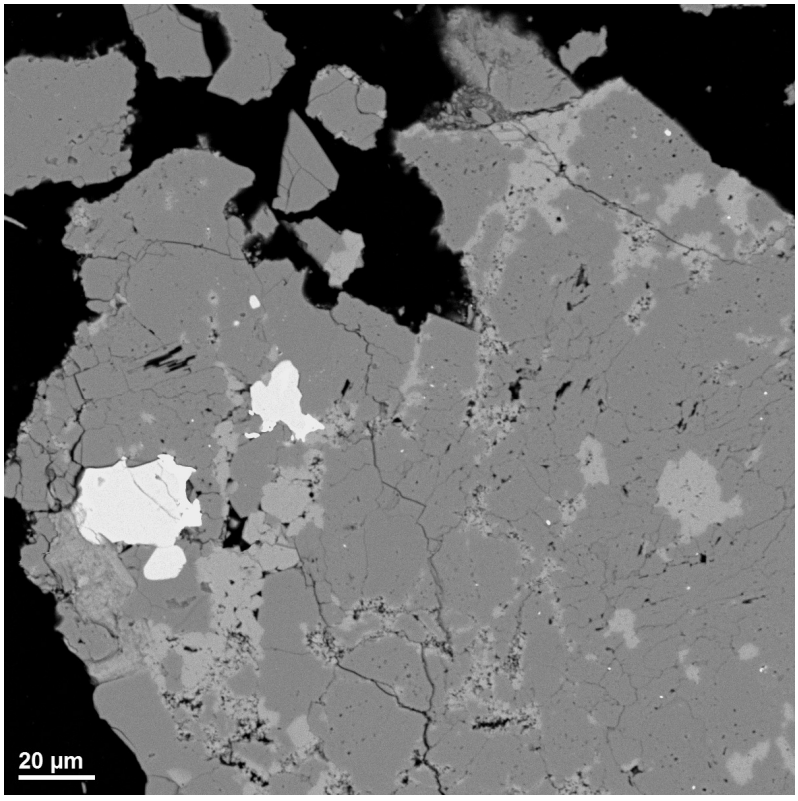

Figure 33: Part of a Fragment Containing K-Feldspar (Medium Grey), Albite (Dark Grey), Quartz (Dark Grey), and Apatite (Light Grey). Thin Mantles of Monazite Occur Along the Borders of the Apatite.

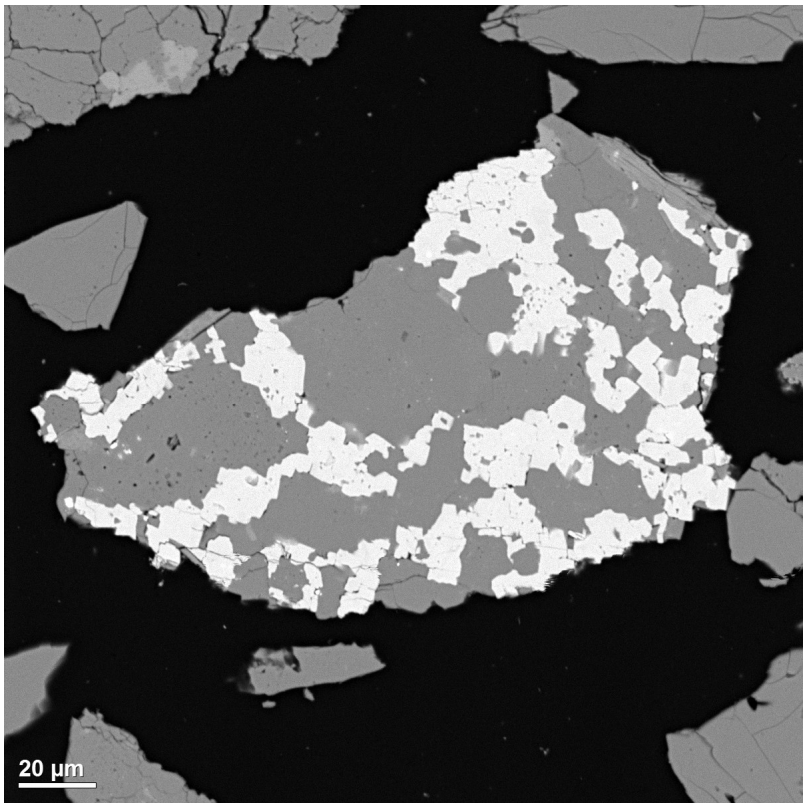

Figure 34: Fragment Consisting of Quartz (Dark Grey) and Fe-Carbonate (Light Grey). A Small Grain of Muscovite (Medium Grey) Occurs Along the Upper Right Edge of the Fragment.

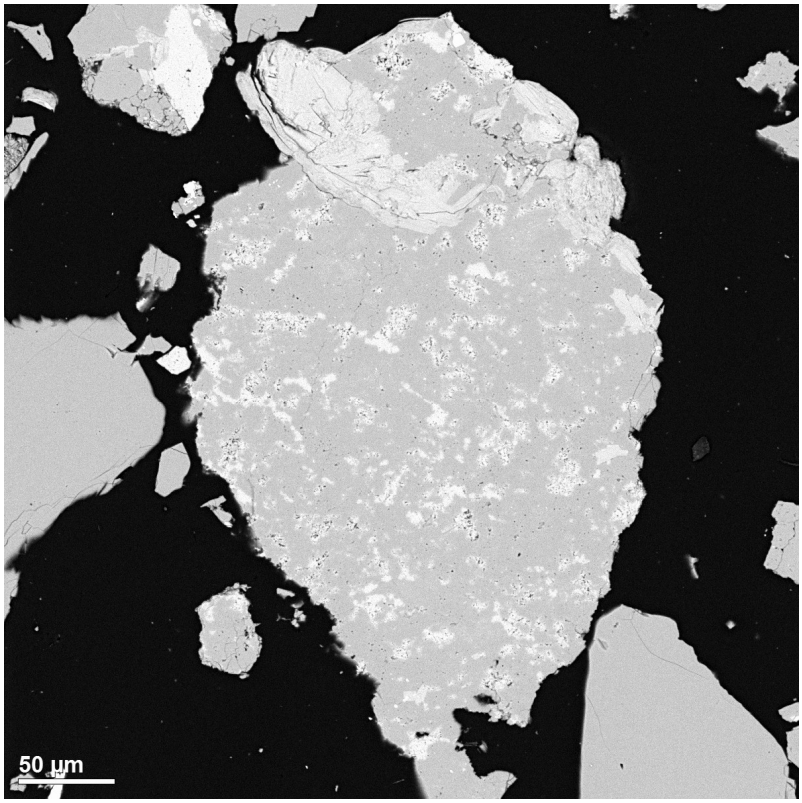

Figure 35: Fragment Consisting of Quartz (Medium Grey) and K-Feldspar (Light Grey), with Muscovite Grains at the Top and Along the Upper Right Edge of the Fragment.

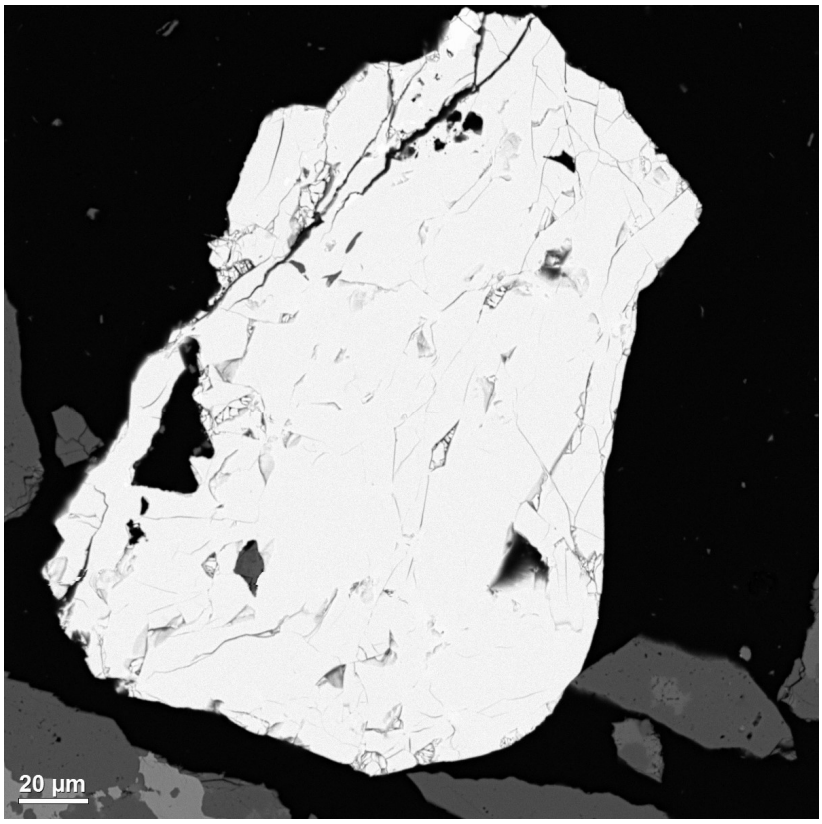

Figure 36: Discrete Grain of Chalcopyrite.

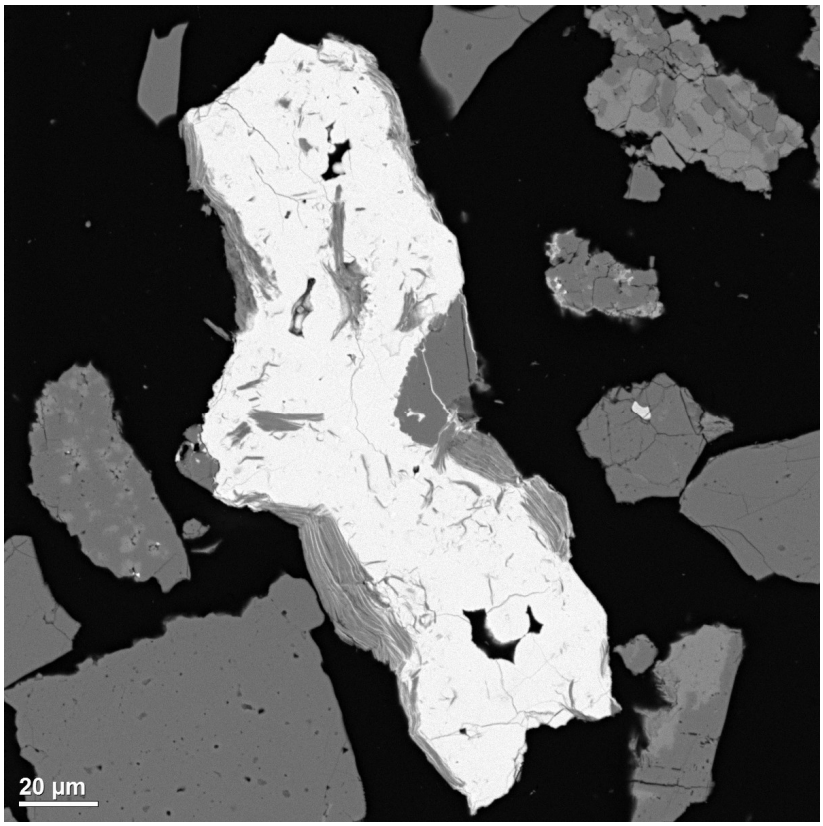

Figure 37: Fragment Consisting of Fe-Carbonate (Light Grey), with Quartz (Dark Grey) and Muscovite (Medium Grey). Fe-Carbonate Also Occurs Along the Cleavages of Some Mica Grains.

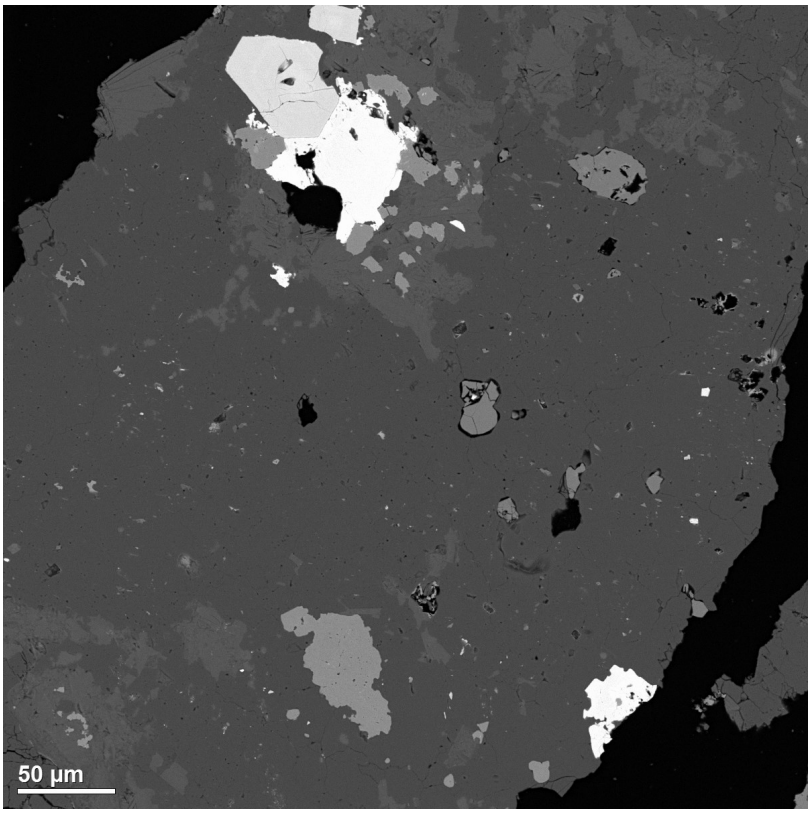

Figure 38: Fragment Consisting of Quartz (Dark Grey) and Muscovite (Medium Grey) with Inclusions of Apatite, Rutile, Zircon, and Xenotime.

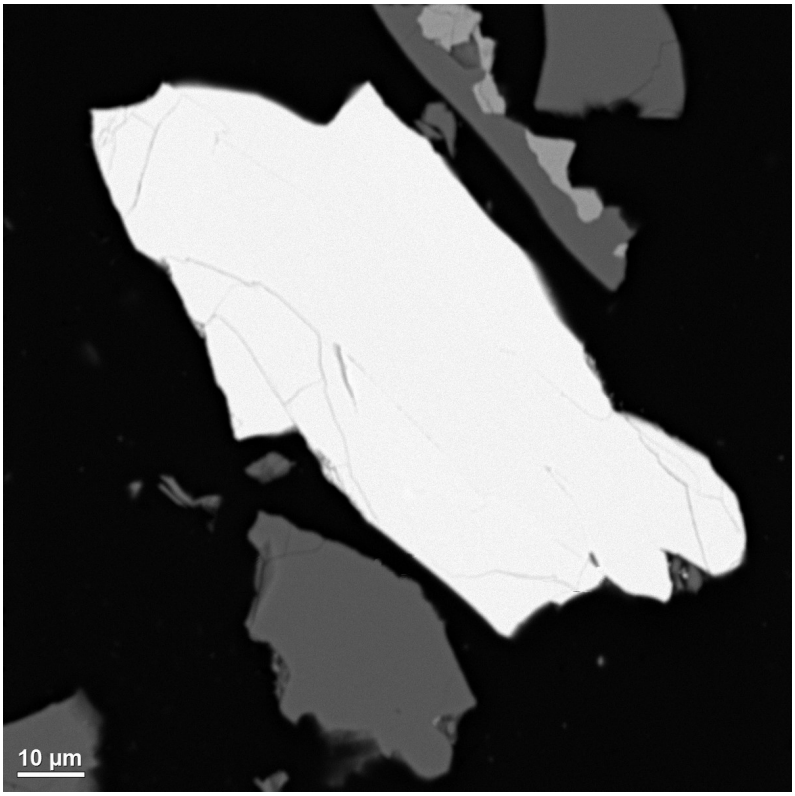

Figure 39: Discrete Pyrite Fragment (White) Surrounded by Small Fragments of Quartz (Dark Grey). The Elongate Quartz Grain at Top Contains Fe-Carbonate (Medium Grey).

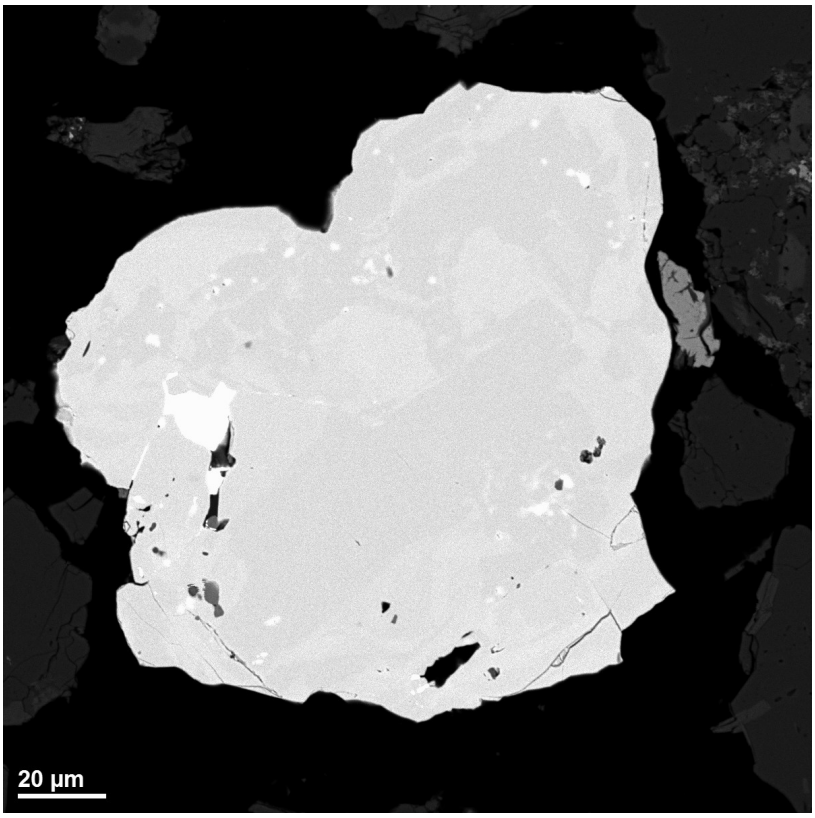

Figure 40: Fragment Consisting of Pyrite with Inclusions of Galena and Chalcopyrite (White). The Slightly Brighter Areas of the Pyrite are Enriched in Arsenic.

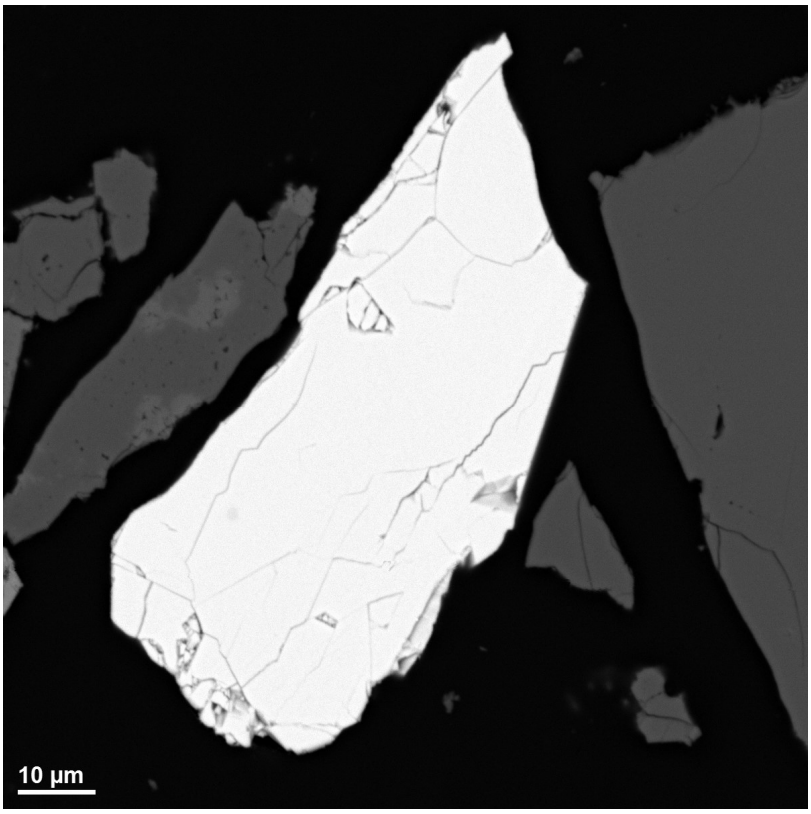

Figure 41: Discrete Fragment of Sphalerite.

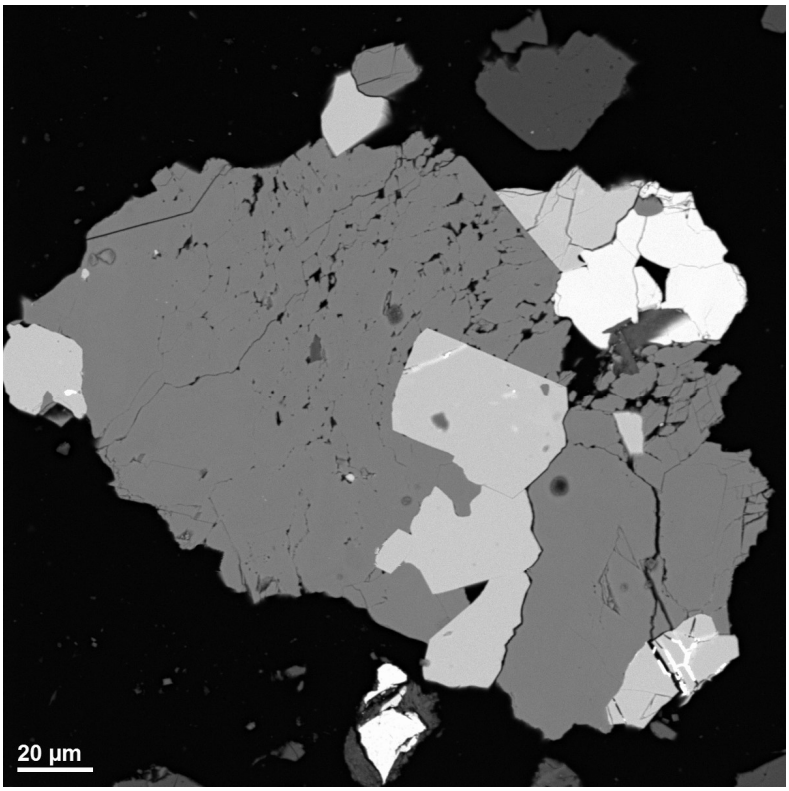

Figure 42: Fragment of Fe-Carbonate (Dark Grey) with Pyrite (Medium Grey) and Sphalerite (Light Grey). The Small Pyrite in the Lower Right Portion of the Fragment has Thin Veins of Galena (White).

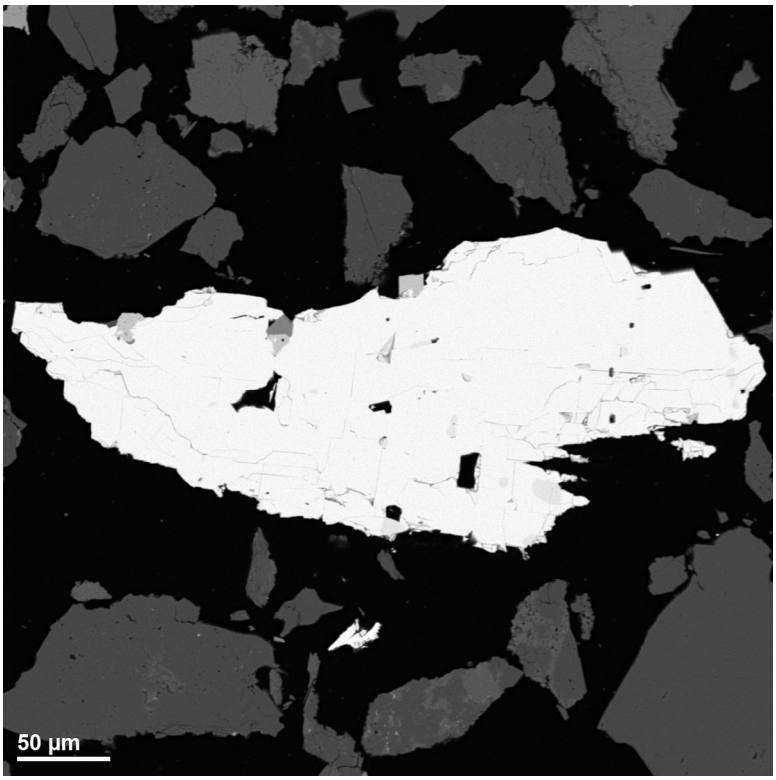

Figure 43: Discrete, Irregular Fragment of Sphalerite. Small Grains of Pyrite and Fe-Carbonate Occur Along the Upper Edge of the Fragment.

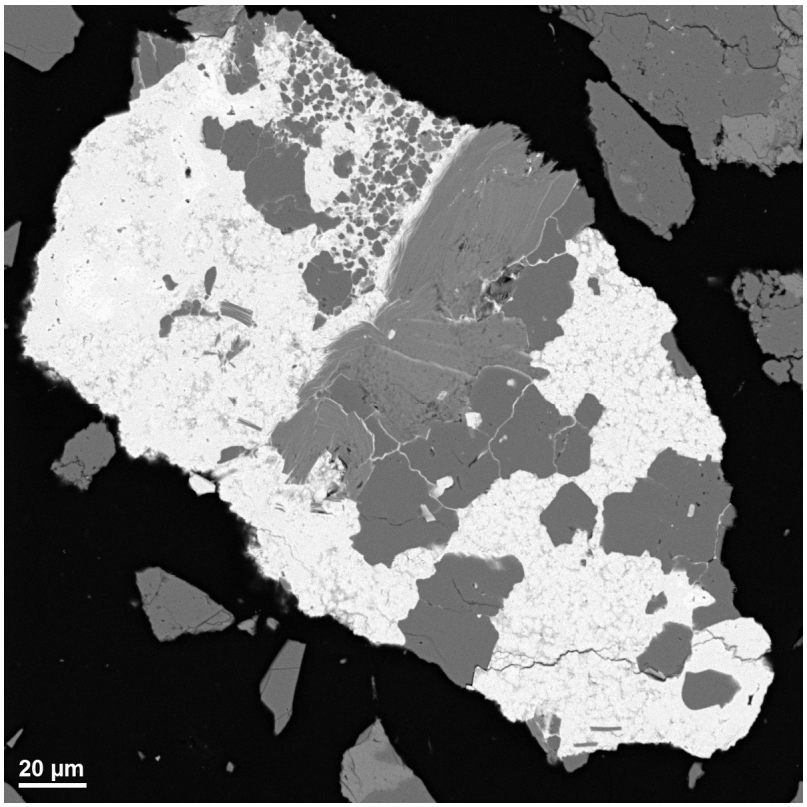

Figure 44: Fragment of Fe-Carbonate (Light Grey) Together with Muscovite (Medium Grey) and Albite (Dark Grey).

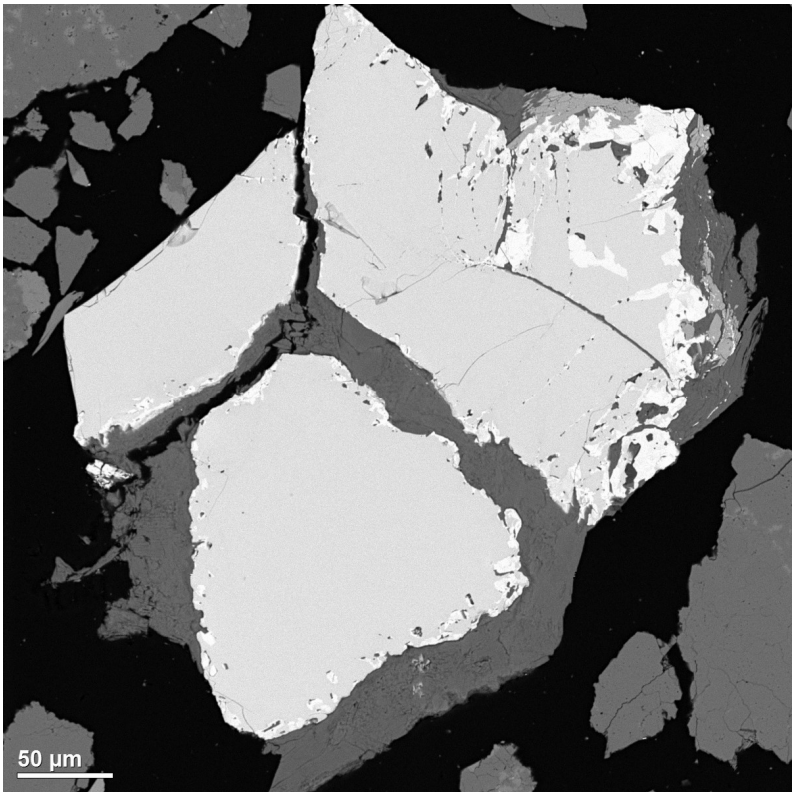

Figure 45: Cr-Rich Spinel Surrounded by Mg-Chlorite. The Brighter Areas of the Spinel are Enriched in Chromium.

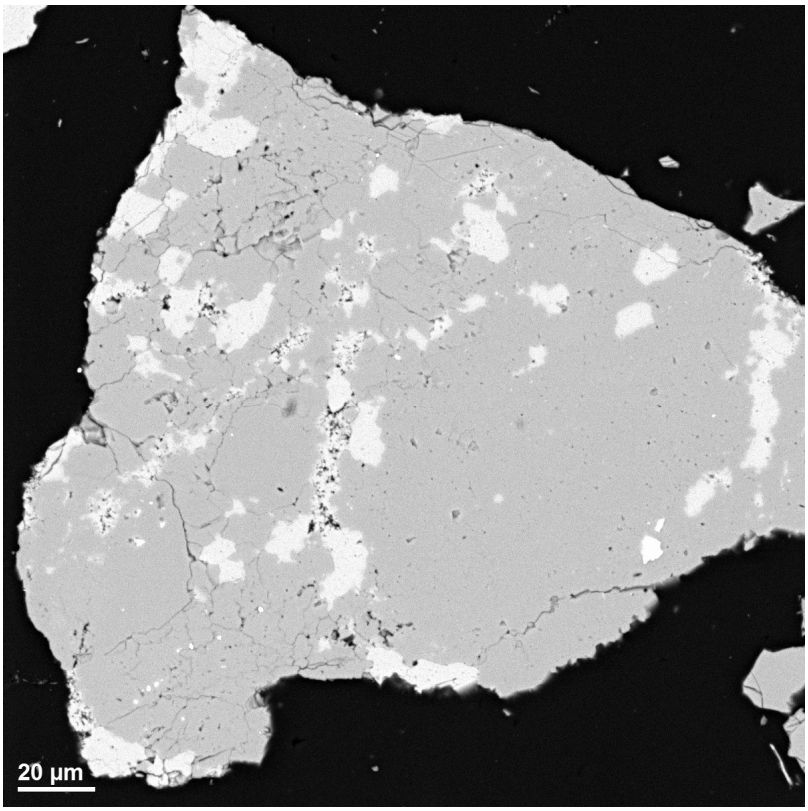

Figure 46: Silicate Fragment Consisting of K-Feldspar (Light Grey), Quartz and Albite (Medium Grey). Note that Quartz and Albite Have Approximately the Same Brightness.

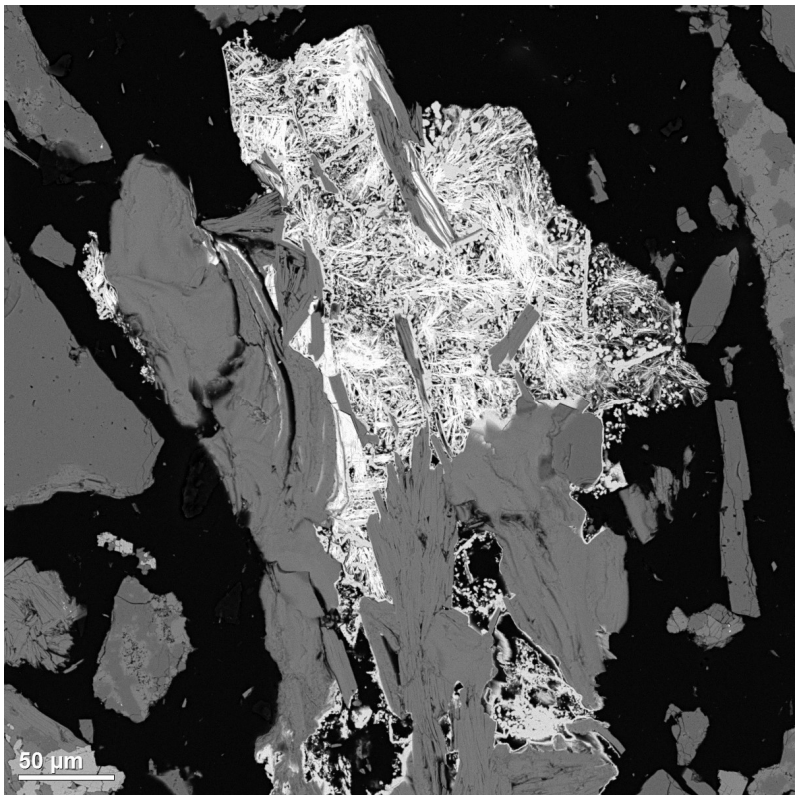

Figure 47: Muscovite Fragment (Medium Grey) with Needle-Like Intergrowth of Fe-Hydroxide (White). The Hydroxide Contains Minor Amounts of Pb, K, Ca, Mg, and Al.

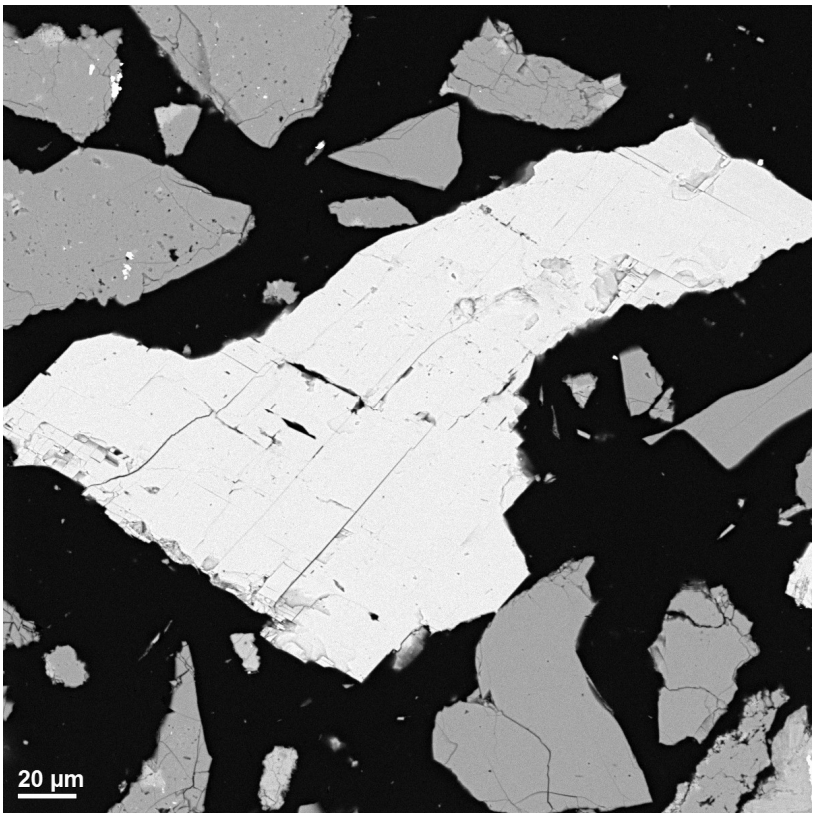

Figure 48: Discrete Fragment of Ca-Carbonate, with Minor Mg and Fe. The Composition on an Atomic Basis is Approximately $Ca_{50}Fe_{33}Mg_{15}Mn_2$.

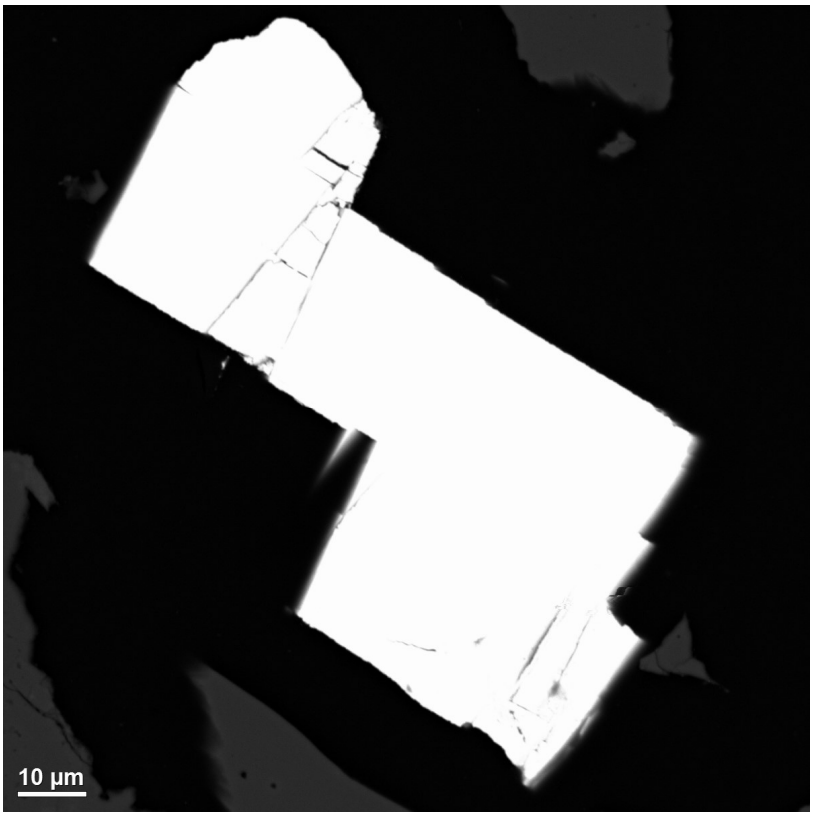

Figure 49: Discrete Fragment of Galena.

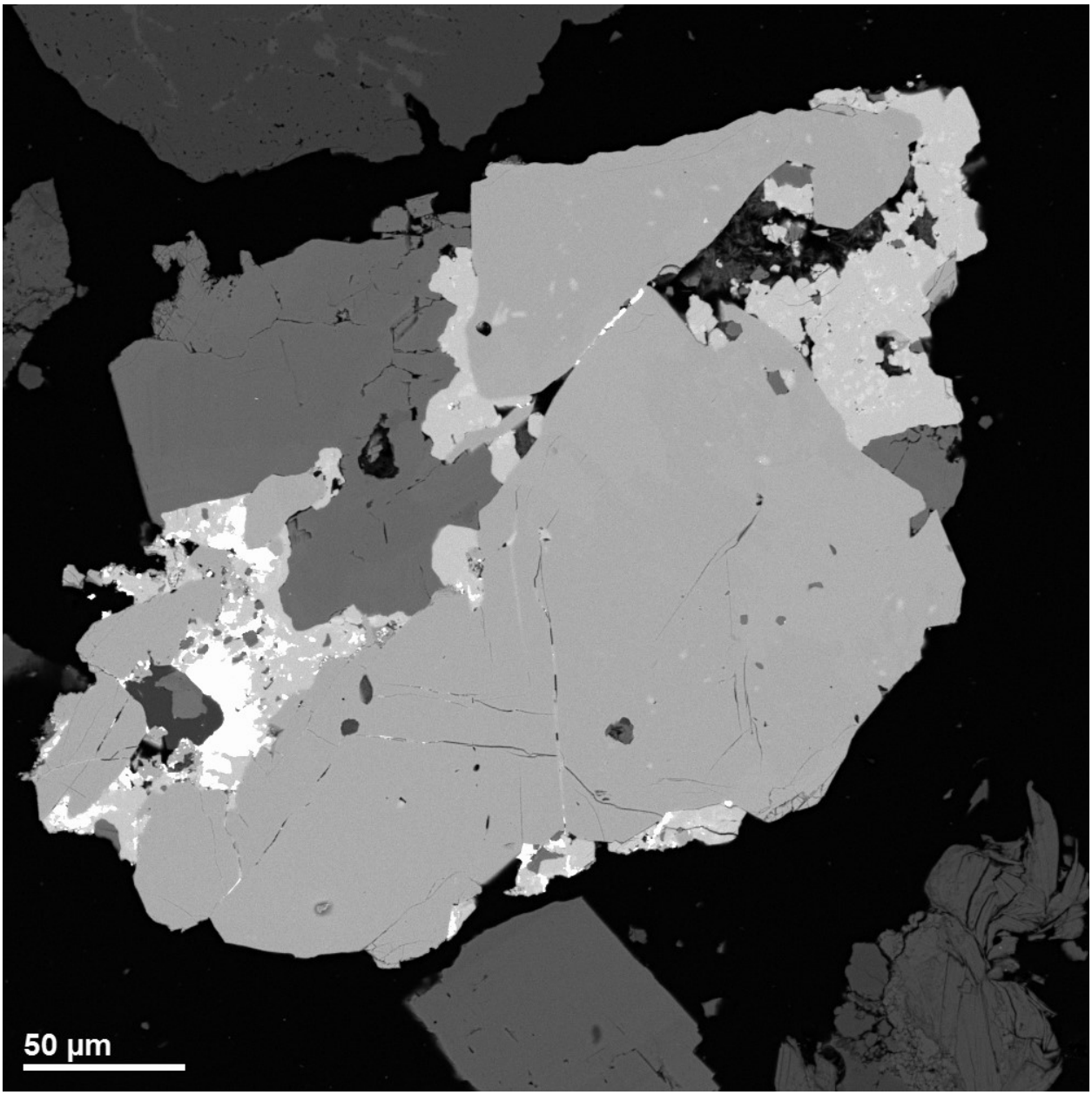

Figure 50: Sulphide Fragment with Fe-Carbonate (Dark Grey), Pyrite (Medium Grey), Chalcopyrite (Light Grey) and Galena (White). The Lighter Inclusions in Chalcopyrite are Sphalerite. The Lighter Inclusions in Pyrite are Chalcopyrite.

Backscattered Electron Images on LGV Rhyolite Pulp Sample

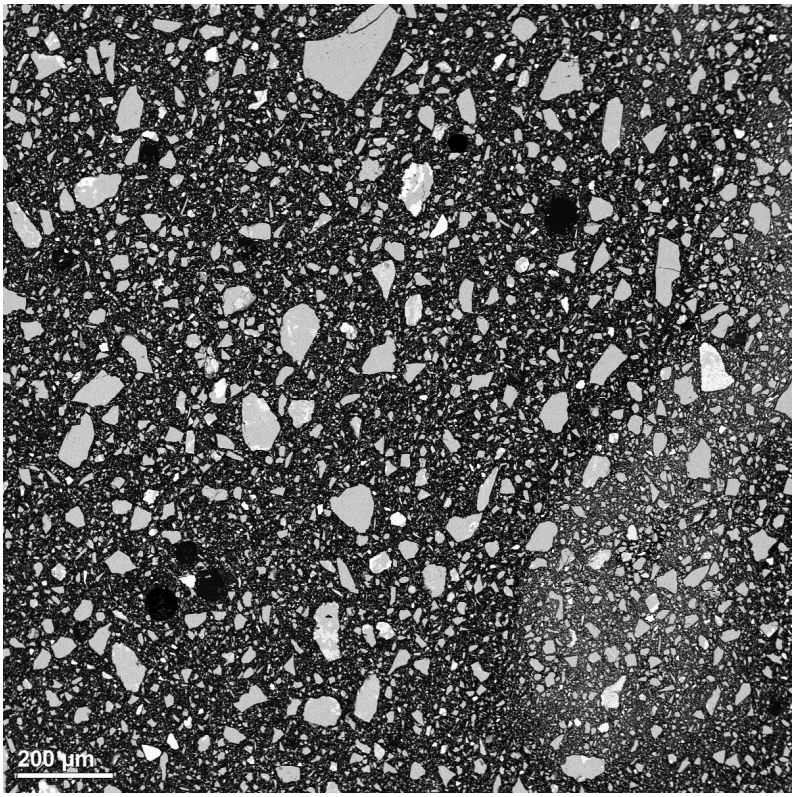

Figure 51: Low Magnification Overview.

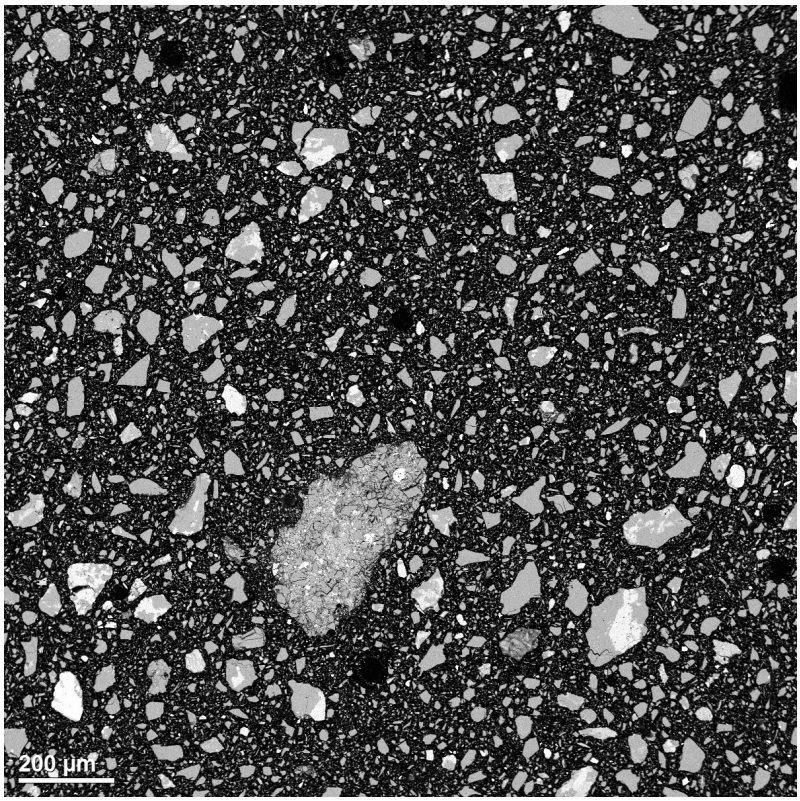

Figure 52: Low Magnification Overview.

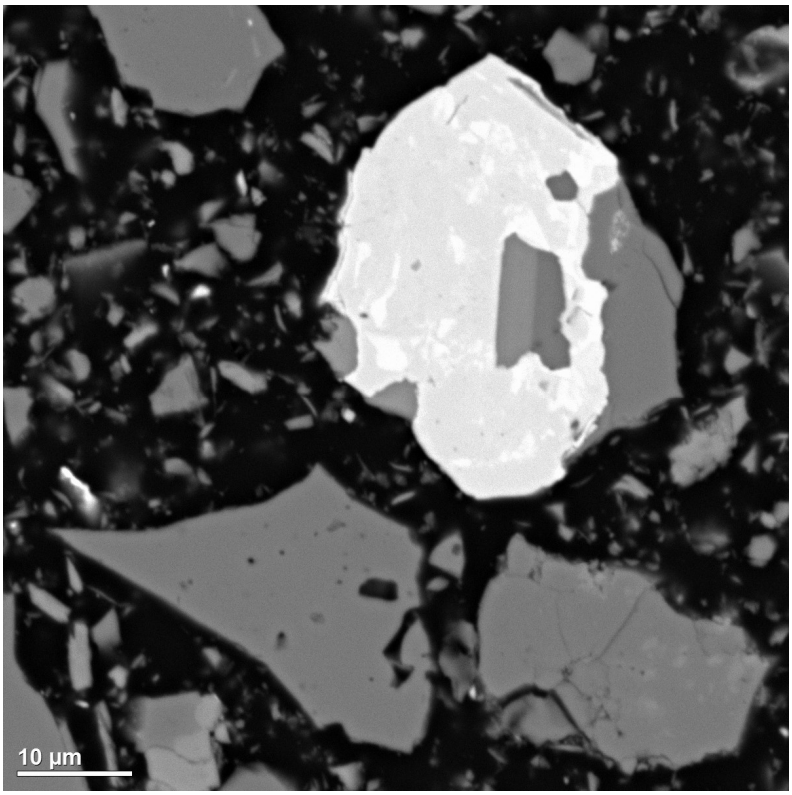

Figure 53: Fragments Consisting of Rutile, Muscovite, and Quartz (Top), Quartz (Bottom Left), and Quartz with Fine K-Feldspar Inclusions (Bottom Right). Brighter Areas in the Rutile are Enriched in Tungsten and Niobium.

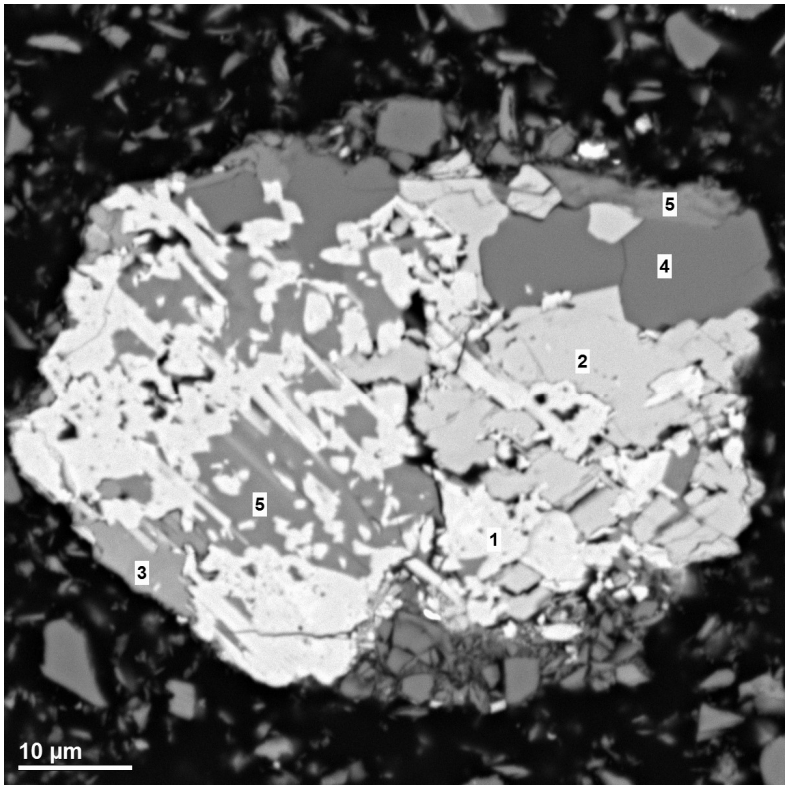

Figure 54: Fragment Consisting of 1) Rutile, 2) Fe (Mg)-Carbonate, 3) Ca (Mg,Fe)-Carbonate, 4) Albite, and 5) Muscovite.

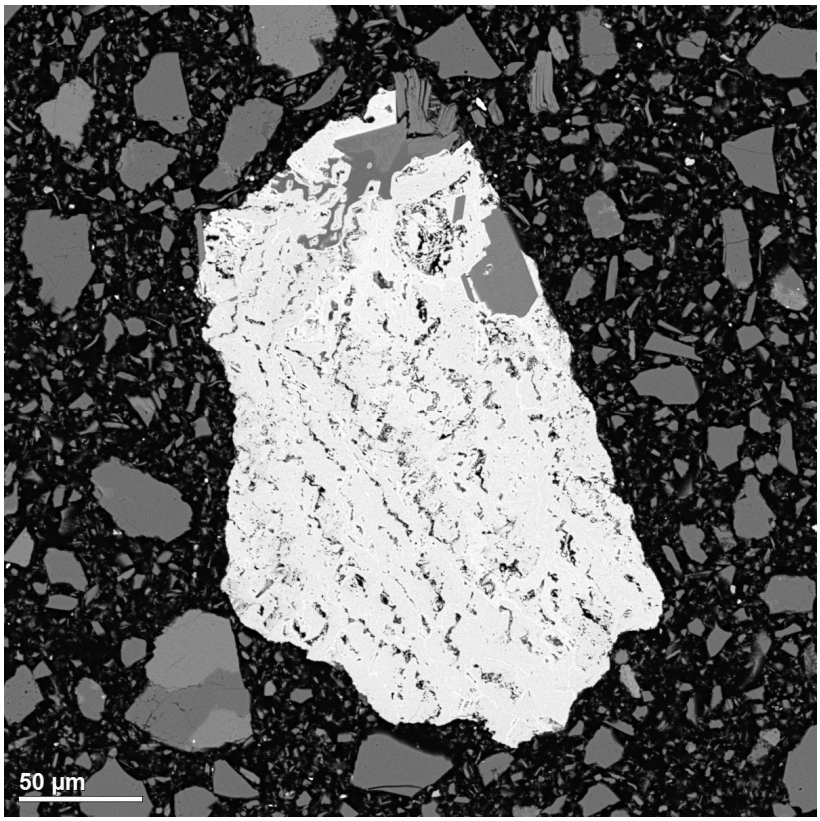

Figure 55: Fragment of Fe-Oxide (Bright Grey) Together with Muscovite (Medium Grey).

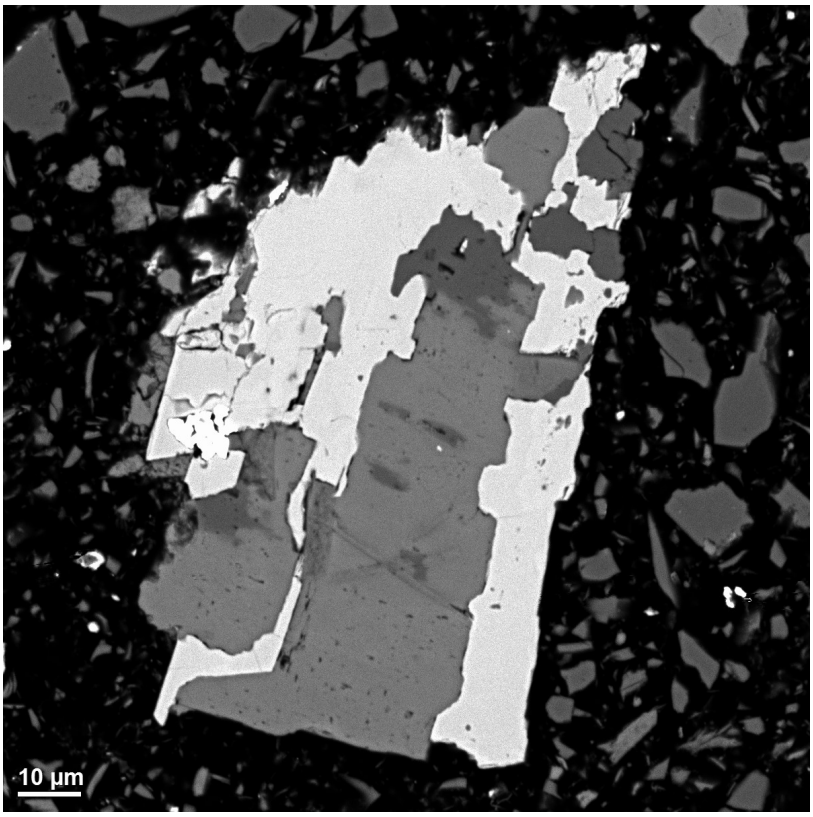

Figure 56: Fragment of Fe (Mg)-Carbonate (Medium Grey), K-Feldspar (Light Grey; Right), Albite and Very Fine Monazite (White, at Left).

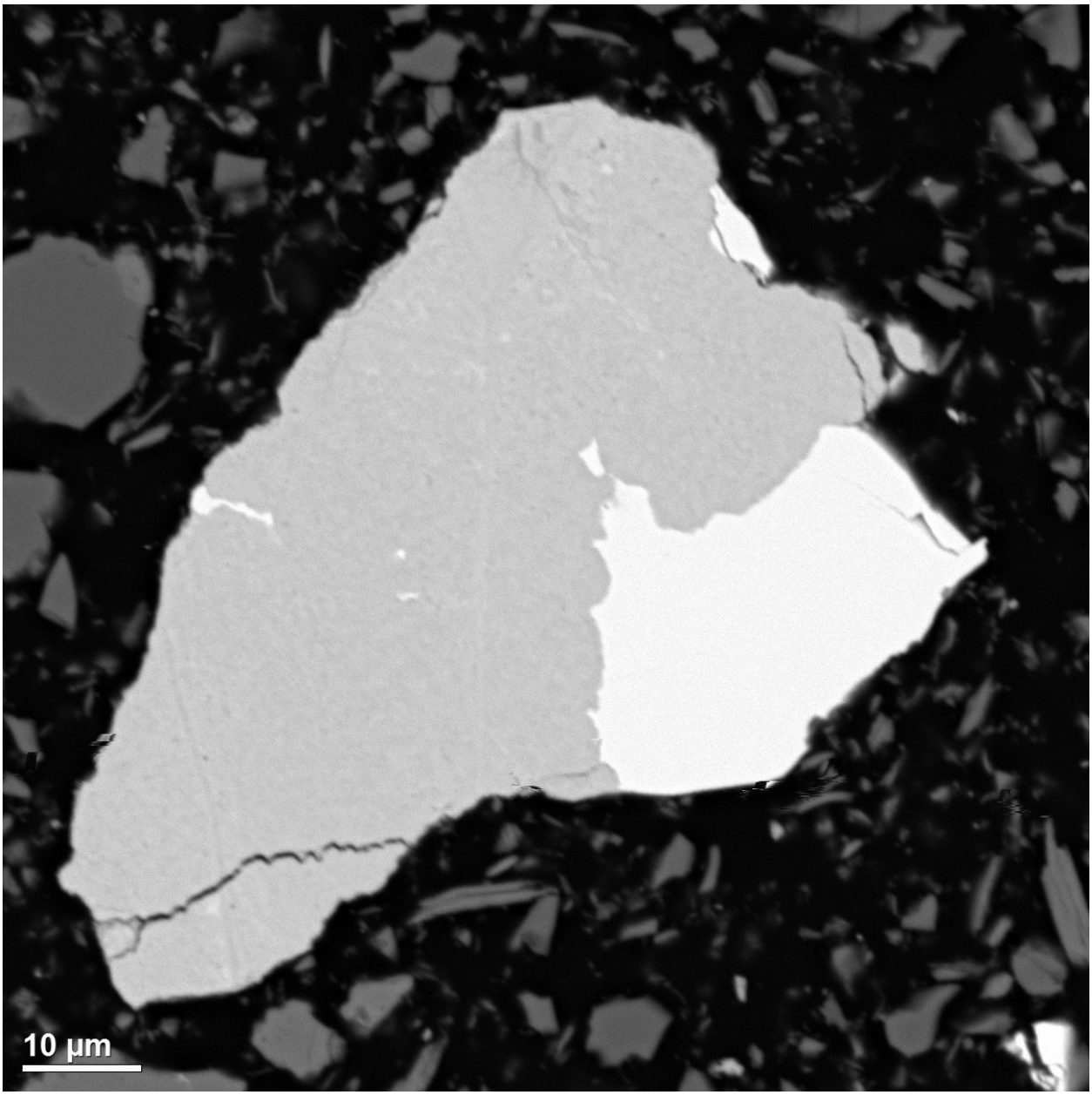

Figure 57: Fragment Consisting of Fe-Oxide (Medium Grey; Left) and Pyrite (White; Right).